中国科学技术大学

学士学位论文

具有赝磁场的石墨烯中的复合费米子液体理论

作者姓名: 胡啸东

学科专业: 理论物理

导师姓名: 副教授 刘国柱　副教授 吴英海

完成时间: 二○一八年五月二十三日

University of Science and Technology of China

A dissertation for bachelor's degree

Composite Fermion Liquid in Graphene with Pseudo-magnetic Field

Author: Xiaodong Hu

Speciality: Theoretical Physics

Supervisors: Prof. Guo-Zhu Liu, Prof. Ying-Hai Wu

Finished time: May 23, 2018

Acknowledgements

I cherished the final time in USTC and was fortunately being supervised by two teachers during my research on this problem. I appreciated the theoretical guidance of Prof. Guo-Zhu Liu in USTC, without whom I cannot get out of mire when recovering the tedious computation details of HLR's theory during my winter vacation. I benefit a lot from his guidance of functional path integral formalism, which accelerated my understanding of the relevant chapters of Altland&Simons's book and calculation of the matrix element of polarization tensor. His course *Quantum Many Body Physics* also endowed me a solid foundation on theoretical condensed matter physics. I also appreciated the physical instruction from Prof. Ying-Hai Wu in HUST. Weekly exchanges with him cleared all my vagueness about the physical picture of the $\mathcal{K}$-matrix with high degeneracy and multi-layer flux attachment. These discussions also prevented me from the potential deviation from the mainline — once I naively insisted that we should develop a Fermionic Chern-Simons theory for massless Dirac fermions, it was his distinct demonstration terminated my divergent thoughts and helped me re-focus on our project.

Moreover, frequent academic exchanges with my best friend Zhihao Zhang galvanized a logic derivation to the singular gauge transformation and Chern-Simons action. In fact, apart from my dissertation, whenever I look back my life in USTC, there was always a figure of him residing in my fragments of memory. I believe our intimate friendship and relation of mutual promotion will extend to the rest of life. Academic debates with my roommate Shu-xuan Wang also helped me clarify some subtle concepts. Frankly, the first time I observed the close relation of functional mean-field methods and spontaneous symmetry breaking happened in the dormitory. An anonymous answerer on Chinese Q&A website `zhihu` also provided me with some information about half-filling FQHE at the frontier of research. So here I sincerely express my gratitudes to them as well.

Contents

中文内容摘要 · · · · · · · · · · 2
英文内容摘要 · · · · · · · · · · 3

Chapter 1 Introduction · · · · · · · · · · 4
1.1 Historical Review of Experimental Results · · · · · · · · · · 4
1.2 Composite Fermions and Chern-Simons Theory · · · · · · · · · · 5
1.2.1 Single-layer Fermion Chern-Simons Theory · · · · · · · · · · 5
1.2.2 Multi-layer Fermionic Chern-Simons Theory · · · · · · · · · · 6
1.3 Symmetrical Strain on Graphene · · · · · · · · · · 7

Chapter 2 SU(2) Fermionic Chern-Simons Field Theory of the Effective Non-relativistic Fermions in Graphene · · · · · · · · · · 9
2.1 Graphene in Strong Magnetic Field · · · · · · · · · · 9
2.1.1 Relativistic or Non-relativistic · · · · · · · · · · 9
2.1.2 Coulomb Interaction on Lowest LL · · · · · · · · · · 10
2.2 Introduction of Chern-Simons Fields and K-matrix · · · · · · · · · · 12
2.3 Action of Fermionic Chern-Simons Theory · · · · · · · · · · 15
2.4 Mean-field Approximation and Gaussian Fluctuation · · · · · · · · · · 17
2.5 Electromagnetic Response Tensor · · · · · · · · · · 21

Chapter 3 Discussions And Outlooks · · · · · · · · · · 25
3.1 Remarks on Non-relativistic Fermionic Theory · · · · · · · · · · 25
3.2 Similarities and Discrepancies with Spin Unpolarized Fermionic Chern-Simons Theory · · · · · · · · · · 25
3.3 Outlooks · · · · · · · · · · 26
Appendix A Proof of the General Form of K-matrix · · · · · · · · · · 28
Appendix B Validy of Diagonal Polarization Tensor at Long Wave-length Limit 30
Appendix C Evaluation of Polarization Tensor and Excitation Spectrum under Long Wave-length Limit · · · · · · · · · · 31
C.1 Static Limit $\omega = 0$ · · · · · · · · · · 31
C.2 Low Frequency Limit $\omega \ll qp_F/m$ · · · · · · · · · · 33
C.3 Large Frequency $\omega \gg qk_F/m$ · · · · · · · · · · 37
Bibliography · · · · · · · · · · 38

中文内容摘要

我们在本文中发展了一套研究石墨烯中朗道填充因子 $\nu = 1/2$ 且非极化填充的有效理论，计算了它在由扭曲石墨烯造成的反向赝磁场激励下的电磁响应与霍尔电导。

在部分填充的情况下，由于费米子被限制在最低朗道能级，当我们将原来的万尼尔表象下的场算符变换到朗道能级波函数的表象上时，发现子格点简并度与谷简并度合二为一，故而根据本征函数的性质，可以用有质量的二次型色散关系的准粒子哈密顿量来有效地描述石墨烯中的无质量狄拉克费米子。而尽管表象变换后一般能级的库伦相互作用变得极为复杂，对于我们关注的最低朗道能级的情况，计算后依旧可以采用原来的相互作用形式。因此我们的哈密顿量与正常的半导体单分量分数量子霍尔效应的差异仅仅在于谷简并带来的多分量。

基于非极化填充的多分量 Chern-Simon 理论，我们在反向赝磁场下计算了电磁响应张量。发现它的激发谱，无论是有能隙的分数量子霍尔态激发，还是无能隙的激发，都与正常半填充因子分数量子霍尔效应的结果一模一样；但是在我们的独特激励下，它的径向响应变为正常半填充因子情况的两倍，而静态横向电导精确等于零。通过表面声学波实验，可以验证石墨烯在分数填充因子下我们的非相对论费米型 Chern-Simons 理论的有效性。

关键词：石墨烯；赝磁场；分数量子霍尔效应；费米型 Chern-Simons 理论

Abstract

We develop an effective theory of unpolarized states in half-filled graphene, studying the electromagnetic response and Hall conductance under the pseudo-magnetic field induced by symmetrical strain on graphene.

In the case of partial filling, when we perform the representation transformation from Wannier function to Landau Level (LL) wave functions, one finds that the valley degeneracy coincides with the sublattice degeneracy at the lowest LL. So in terms of the form of eigen functions, we can make use of the Hamiltonian of massive particles with parabola dispersion relation to describe the massless Dirac fermions in graphene. Although the expression of Coulomb interaction becomes extremely complicated after transformation of representation for general LL, in the situation what we concern with, where only the lowest LL is occupied, the original form of interaction never becomes futile after computation. Thus the only difference of our theory to that of fraction quantum Hall effects (FQHE) in usual semiconductors comes from the more freedoms brought by the valley degeneracy.

Based on the fermionic Chern-Simons theory of unpolarized states, we calculate the electromagnetic response tensor under the stimulus of opposite pseudomagnetic field and find that the excitation spectrum, whatever gapped FQHE states or gapless one, coincides with that of usual partially filled FQHE. But our special stimulus makes the longitudinal response double and the static transverse conductance vanish. The effectiveness of our theory can be confirmed by the accurate surface acoustic wave experiments.

Key Words: Graphene; Pseudo-magnetic Field; Fractional Quantum Hall Effect; Fermionic Chern-Simons Theory

Chapter 1 Introduction

1.1 Historical Review of Experimental Results

The integer quantum hall effect (IQHE) was first observed in two-dimensional electron gas (2DEG) electrostatically induced by metallic gate valtage on Silicon MOSFET or by modulation dopped GaAs-AlGaAs heterostructure by von Klitzing [1-3]. Stark contrast is observed on the stepwise dependence on strong magnetic field, as compared to a linear dependence as in classical Hall effect. Those step Hall resistances, or plateaus, quantized with extreme high resolution as $\frac{h}{ne^2}$ with an *integer* n, while the corresponding longitudinal resistance drops sharply to zero in the meanwhile. The high resolution even made quantum Hall effect (QHE) as the resistance calibration standard since 1990.

Two years after the first observation of IQHE, fractional quantum Hall effect (FQHE) was discovered by Tsui, Stormer and Gossard [4-5] in a much lower temperature and higher magnetic fields environment on a higher mobility 2DEG of Si-dopped GaAs-AlGaAs heterojunctions. FQHE possesses an analogous characteristic as QHE, except that the quantized Hall resistance is $\frac{h}{e^2}$ divided by a *fraction*. The first observed fraction is $\nu = 1/3$ and about 100 fractional quantum Hall states have been observed so far [6]. Most of these fractions are of odd denominator, but the existence of even denominator FQHE states like $\nu = 1/2, 5/2$ aroused huge theoretical interests in this field.

Regardless how the 2DEG is formed, gauge invariance and impurity-induced localization [2, 7] are widely accepted as the cause of IQHE①, and interplay of kinetic energy and interaction results in FQHE [8]. So besides the familiar heterostructures like Si-MOSEFT or dopped GaAs-AlGaAs, Graphene and other two-dimensional materials are also believed to host IQHE and FQHE. And experimentalists did find a slightly distinct anomalous quantized Hall conductance in graphene [9] that $\sigma_{xy} = \pm 4(n + \frac{1}{2})\frac{e^2}{h}$. The factor 4 comes from the spin degeneracy and valley degeneracy of graphene, and the extra translation $1/2$ is ascribed to the presence of the zero mode shared by two Dirac points that does not exist in semiconductor heterostructures.②[10-12].

①TKNN theory [7] also provide one explanation of IQHE.

②Because of the extra existence of $N = 0$ LL at two pair of Dirac points, there would be $2(2N + 1)$ occupied

FQHE in graphene was also found four year latter in a suspended graphene with high mobility comparable to some good quality 2DEG in GaAs-AlGaAs heterostructure in [13-14]. Both groups of Du *et al.* and Dean *el al.* merely found odd denominator fraction states. But in 2014, even denominator states are also observed in suspended graphene [15]. Therefore, motivated by rich physics hidden in even denominator FQHE in GaAs, it's valuable to study the electromagnetic transports in graphene with even denominator Landau Level (LL) filling factors as well, particularly, we concentrate on the case of $\nu = 1/2$ in this paper.

1.2 Composite Fermions and Chern-Simons Theory

The concept of *composite fermion* stem from the Jain's famous paper in 1989, in which a mapping between the wave functions of IQHE states and approximate — but extremely good — wave functions for FQHE states is keenly pointed out [16]. This wave function mapping can be regard as attaching an *even* number of vortices of the wave function to each electron, turning it into a "composite" fermion.

Although the idea of composite fermion suffered some resistance from the theoretical community at first, its validity was gradually accepted and the idea was further developed by many groups. S.C. Zhang *et al.* shot to fame with their model of bosonic Chern-Simons theory, in which *odd* number of flux is attached and incompressible excitation of FQHE states are explained by the Ginzberg-Landau theory of symmetry breaking [17]. Approaches of fractional statistics and Chern-Simons field also culminate the field of anyon superconductivity [18-19] for a time.

1.2.1 Single-layer Fermion Chern-Simons Theory

The fermionic Chern-Simons field theory proposed by Lopez and Fradkin in [20] comes to epitomize the development of field theory formalism on FQHE, providing a systematic (or at least semi-systematic) perturbation calculations of quantities such as longitudinal and transverse conductivities that are experimentally measurable. And formal study of the relation of wave function of ground state with the generating function of green function at equal time in [21] enable Fradkin to bridge the field theory formal-

states transferred from one edge to another.

ism to Jain's trial series of incompressible FQHE wave functions. Shortly thereafter, the half-filling state is also well described by Halperin, Lee, and Read's famous work [22] (known as HLR) with this approach, surprisingly indicating that unlike incompressible FQHE states with odd denominators, the even denominator states like $\nu = \frac{1}{2}, \frac{1}{4}$ are rather compressible and Fermi-liquid-like①.

1.2.2 Multi-layer Fermionic Chern-Simons Theory

If one more freedoms are added in Fermionic Chern-Simons theory, a richer variety of states is believed to emerge. And two obvious situations that can be described by this multi-component theory are systems in which the spin freedom is no longer frozen by Zeeman effect and the multi-layer 2DEG coupled together. In fact, liberating the spin degree of electrons in GaAs-AlGaAs helps in interpreting the unconventional $\nu = 5/2$ FQHE state observed in experiments②, which once cast doubt on Fermionic Chern-Simons Theory that predicts FQHE states with only odd denominators $\nu = \frac{p}{2np+1}$. In the application of multi-layer two dimensional systems (2DES), however, the interplay of intra-layer and inter-layer Coulomb interaction give rise to more interesting physics. Half-filled FQHE has already been observed in double layer electron system in [28], but is proven to be a compressible Fermi liquid state for a single layer in theoretical constructions [23] and in energy gaps determination experiment of prominent sequences of FQHE states [29] at filling factor $\nu = p/(2p \pm 1)$ around $\nu = 1/2$.

Thus, together with the natural four-fold energy spectrum of graphene and preceding theoretical development, we decide to utilize the multi-layer Fermionic Chern-Simons theory to study the hall-filled state in graphene as well. Luckily enough, much preceding theoretical breakthrough has paved the way to this direction. For non-relativistic particles, Fradkin and Lopez first considered double layer Fermionic Chern-Simons theory in [30], and was extended to arbitrarily polarized QHE states by Mandal *et al.* in

①More precisely, the behavior of *infrared divergence* of the effective mass of composite fermions [23] reveals that even denominator states are *marginal Fermi liquid*. But theoretical framework of normal Fermi liquid aptly fit the physical picture of this system with just a slight but reasonable modification of the model.

②Haldane and Rezayi's once constructed celebrated spin unpolarized states in [24] to explain $\nu = 5/2$ FQHE states, but was proven to be asymptotic states in the vicinity of the critical point of phase transition with gapless excitation in the bulk [25], while the Pfaffian states proposed by Moore and Read in [26] aptly matches the weak-pairing phase in [25] as was numerically support by [27].

[31]. For massless Dirac fermions, Modak *et al.* classify states with discussion of the $\mathcal{K}$-matrix with spin, valley and mixed polarizations in [32], Pyatkovskiy *et al.* gives cumbersome computation details of dynamic polarization tensor in [33] and Fräßdorf culminate this direction by giving a general expression of response matrix as Fradkin them did in Keldysh formalism.

1.3 Symmetrical Strain on Graphene

Attempts of imposing strain on graphene started started from early age. For instance, uniaxial strain is applied to tune the characteristics of Raman spectrum and open the band gap [34-35]. However, they did not arouse much attention until Manes's general revelation of the relation of the model-independent coupling between electrons and long-wavelength acoustic and optical phonons, which can be applied in describing elastic strains in terms of effective pseudomagnetic fields in monolayer graphene [36-37]. Manes proves that an arbitrary two-dimensional strain field $u(\boldsymbol{r})$ could lead to a pseudo gauge field

$$\boldsymbol{A'} = \frac{t\beta}{ev_F}\begin{pmatrix} u_{xx} - u_{yy} \\ -2u_{xy} \end{pmatrix}, \tag{1.1}$$

where t is the nearest-neighbor hopping parameter, $\beta = -\partial \ln t/\partial \ln a$ is the dimensionless coupling parameter in description of lattice deformation. Another theoretical elegantly prediction of this pseudomagnetic field can be made through direct comparison of the Hamiltonian of massless Dirac fermion in a uniform external magnetic field

$$\hat{H}^2_{\text{flat}} = v_F^2 \delta^{ij} \hat{\pi}_i \hat{\pi}_j + e\hbar v_F^2 B \sigma_3 \tag{1.2}$$

to that of Dirac fermions in *curved two-dimensional manifold* [38]

$$\begin{aligned} \hat{H}^2_{\text{curved}} &= -\nabla_i g^{ij} \nabla_j - g^{-1/4}(\partial_i \sqrt{g} \partial_j g^{-1/4}) + \frac{1}{4}R = \cdots \\ &\sim \delta^{ij} \hat{\Pi}_i \hat{\Pi}_j + \frac{R}{12}\mathbb{1} + \frac{R}{6}\hat{L}^2 \end{aligned}$$

such that

$$|\boldsymbol{B'}| = \frac{\hbar R}{4e}, \tag{1.3}$$

where R is the scalar Riemann curvature of corrugated graphene, $\hat{\pi}_i$ is the flat kinetic momentum $\hat{\pi}_i = \hat{p}_i + \frac{eB}{2} x_j \varepsilon_{ji}$, $\hat{\Pi}_i$ is the curved kinetic momentum , and $\hat{L}$ is the curved

angular momentum.

Guinea *et al.*'s following realization of pseudomagnetic QHE [39] without help of the external magnetic fields but this strain-induced one, pushed this hot spot to new heights. Through putting the graphene sample on a corrugated substrate surface, Guinea *et al.* achieve to impose a small triangular symmetrical strain[①] to the honeycomb lattice and obtain an extremely high (about $40\mathrm{T}$) but nearly uniform psuedomagnetic fields in the first Brillouin Zone, which can be read form the observed Landau levels. Detailed numerically confirmation is also studied by Verbiest in [40]. What makes this pseudomagnetic field outstanding from the usual probing magnetic fields is that **this strain-induced field *flips around the two Dirac point*, K and K', and the counter-propagating edge states among two valleys share exactly the same picture as quantum spin Hall effect (QSHE)** in [41].

In light of the strength of this pseudomagnetic field and adjustable dopping rate, we believe that the feature of massless Dirac fermions and opposite direction of pseudomagnetic fields make the electromagnetic response valuable to study.

[①]The triangular symmetrical strain is solved from the partial differential equation of (1.1) by letting $\boldsymbol{B'} = \text{const}$.

Chapter 2 SU(2) Fermionic Chern-Simons Field Theory of the Effective Non-relativistic Fermions in Graphene

2.1 Graphene in Strong Magnetic Field

2.1.1 Relativistic or Non-relativistic

The electronic properties of Graphene is well described by the tight binding model [42], in which only nearest neighborhood hopping interaction is considered. Each of the six corner of the hexagonal Brillouin zone protect the time-reversal symmetry [43], but only two of these doubles are inequivalent ones, giving rise to the two-fold valley degeneracy, or pseudospin $\xi = \pm$. Given the celebrated Hamiltonian of graphene in the continuum limit, one can directly write down the Hamiltonian of free Dirac fermions in a strong magnetic field $\boldsymbol{B}$ by simple minimal-coupling principle[①]

$$H_B^\xi = \xi v_F \begin{pmatrix} 0 & \Pi_x - i\Pi_y \\ \Pi_x + i\Pi_y & 0 \end{pmatrix}, \tag{2.1}$$

where v_F is the Fermi velocity and Π_i are the kinetic momentum $\boldsymbol{\Pi} = \boldsymbol{p} + e\boldsymbol{A}$. Through introducing the conjugate ladder operator $a = \frac{\ell_B}{\sqrt{2}}(\Pi_x - i\Pi_y)$ and $a^\dagger = \frac{\ell_B}{\sqrt{2}}(\Pi_x + i\Pi_y)$, the free Hamiltonian (2.1) becomes

$$H_B^\xi = \xi \frac{\sqrt{2} v_F}{\ell_B} \begin{pmatrix} 0 & a \\ a^\dagger & 0 \end{pmatrix}, \tag{2.2}$$

whose eigenstates can be directly solved by squaring (2.2), giving [45-46]

$$\Psi^\xi_{\lambda,(n\neq 0,m)}(\boldsymbol{x}) = \frac{1}{\sqrt{2}} \begin{pmatrix} \psi_{|n|-1,m} \\ \lambda\xi\psi_{|n|,m} \end{pmatrix}, \quad \Psi^\xi_{(0,m)}(\boldsymbol{x}) = \begin{pmatrix} 0 \\ \psi_{0,m} \end{pmatrix}, \tag{2.3}$$

with $\psi_{n,m}(\boldsymbol{x})$ **the eigen function of the Hamiltonian with *quardratic dispersion* in nth LL** with the angular momentum equal to m, i.e., the LL wave function of usual

[①]The minimal-coupling principle in tight binding model is called *Peierls substitution* [44]. Unlike the usual continuous situation, Peierls substitution holds only if the lattice constant a is *much smaller* than the characteristic magnetic length $\ell_B \equiv \sqrt{\frac{\hbar}{eB}}$. And because $a = 0.24\mathrm{nm}$ and $\ell_B \sim 26\mathrm{nm}/\sqrt{B[\mathrm{T}]}$, this condition is fullfilled in graphene for strong magnetic fields.

semiconductor heterojunction like GaAs in Tsui's early experiments [4, 46]

$$\psi_{n,m}(z) = \frac{(-1)^n\sqrt{n!}}{\sqrt{2^{m+n}\pi(m+n)!}} z^m L_n^m\left(\frac{|z|^2}{2}\right) e^{-|z|^2/4},$$

where $z = x - iy$ and $L_n^m(z)$ is the Laguerre polynomials.

Recall that the column of spinors (2.3) represents the two sublattice freedoms. So the distinctive form of $n = 0$ LL wave function, in which one column is always zero, indicates that the valley degeneracy coincides with the sublattice freedoms at the lowest LL, and the two sublattice, B sublattice in the K'-valley while A sublattice in the K-valley, decouple at zero energy [44]. That is, **the effective theory for *free massless Dirac fermions* constrained at the Lowest LL takes exact the same form of *non-relativistic* case but with an extra two-fold pseudospin degeneracy**[①], whose fermionic field operator are denoted as $(\psi_e)_\alpha$ for $\alpha = \uparrow, \downarrow$. Similar to transforming the fields operators from Bloch representation to Wannier representation in Hubburd model [47], the procedure we does above is actually **projecting the free Hamiltonian of Wannier wave function to a new basis of LL wave functions** (and constrain it to the Lowest LL).

2.1.2 Coulomb Interaction on Lowest LL

However, apart from the free parts of Hamiltonian, motivated by the mechanism of fermionic Chern-Simons theory in GaAs-AlGaAs, Coulomb interaction must play a crucial role in formation of incompressible FQHE states obseved in graphene [48], without which the hierachical structure of fraction Hall conductance cannot be consistently explained [8, 20]. In this subsection, we will prove that Coulomb interaction keep its form after basis transformation.

The density operator can be decomposed in the basis of spinor wave functions (2.3)

$$\begin{aligned}\rho^\xi(\boldsymbol{q}) &= \sum_{\lambda,n,m,\lambda',n',m'} e^{-i\boldsymbol{q}\cdot\boldsymbol{r}} \psi^{\xi\dagger}_{\lambda,n,m}\psi^{\xi}_{\lambda',n',m'} a^{\xi\dagger}_{\lambda,n,m} a^{\xi}_{\lambda',n',m'} \\ &= \sum_{\lambda,n,\lambda',n'} \mathcal{F}^{\xi,\xi'}_{\lambda,n,\lambda',n'}(\boldsymbol{q})\widetilde{\rho}^{\xi',\xi}_{\lambda,n,\lambda',n'}(\boldsymbol{q}),\end{aligned}$$

[①]The ambient magnetic field is strong enough to split the energy spectrum into two *nonoverlapping* groups due to Zeeman effects, so we ignore the real spin freedoms of fermions here.

with the reduced density operator

$$\widetilde{\rho}^{\xi',\xi}_{n,m;n'm'}(\boldsymbol{q}) := \sum_{m,m'} \left\langle m \left| e^{-i(\boldsymbol{q}+(\xi-\xi')\boldsymbol{K})\cdot\boldsymbol{R}} \right| m \right\rangle a^{\xi\dagger}_{\lambda,n,m} a^{\xi}_{\lambda',n',m'} \tag{2.4}$$

and the complicated form factor $\mathcal{F}_{\lambda,n,\lambda',n'}$ given in the appendix A of [44]. In terms of this reduced density operator (2.4), Coulomb interaction is written as

$$H_{\text{int}} = \frac{1}{2}\sum_{\boldsymbol{q}} \sum_{\substack{n_1,m_1,\cdots,n_4,m_4 \\ \xi_1,\cdots,\xi_4}} v_{n_1,m_1,\cdots,n_4,m_4} \widetilde{\rho}^{\xi_1,\xi_3}_{n_1,m_1;n_3,m_3}(-\boldsymbol{q}) \widetilde{\rho}^{\xi_4,\xi_4}_{n_2,m_2;n_2,m_2}(\boldsymbol{q}), \tag{2.5}$$

where

$$v_{n_1,m_1,\cdots,n_4,m_4} \equiv \frac{2\pi e^2}{\varepsilon|\boldsymbol{q}|} \mathcal{F}_{n_1,m_1;n_3,m_3}(-\boldsymbol{q}) \mathcal{F}_{n_2,m_2;n_2,m_2}(\boldsymbol{q})$$

Equation (2.5) seems too complex to handle with, but fortunately enough, energy scale comparison of Coulomb interaction to that of inter-gap excitation reveals that[①] **inter-LL interaction may be regarded frozen**, as is shown in Fig. 2.1.

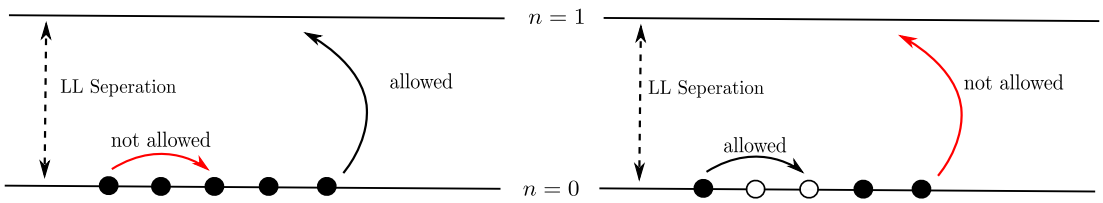

Fig. 2.1 **Comparison of the Filled and Partially Filled LL**. The *inter-LL* excitation is preferred in the left subgraph due to the Pauli exclusion principle of filled LL, while is suppressed in the right subgraph of partial filled LL for the higher energy scale of LL separation comparing with intra-LL interaction.

Under this approximation, (2.5) becomes a neat form of [49-50]

$$H_n = \frac{1}{2}\sum_{\boldsymbol{q}} v_n(\boldsymbol{q}) \widetilde{\rho}(-\boldsymbol{q}) \widetilde{\rho}(\boldsymbol{q}), \tag{2.6}$$

with the simple effective interaction potential

$$v_n(\boldsymbol{q}) = \frac{2\pi e^2}{\varepsilon|\boldsymbol{q}|} \mathcal{F}_n^2(\boldsymbol{q}),$$

[①]Coulomb interaction can be evaluated with the characteristic cyclotron radius $R_C = \ell_B\sqrt{2n+1}$ by $E \sim e^2\varepsilon R_c$, which is much smaller than Landau Level spacing

$$\Delta_n = \sqrt{2}\frac{\hbar v_F}{\ell_B}(\sqrt{n+1} - \sqrt{n})$$

for all $n > 0$ because

$$E/\Delta_n \sim f(n)\frac{e^2}{\hbar v_F} \ll 1.$$

and the former factors [51]

$$\mathcal{F}_n(\boldsymbol{q}) = \frac{1}{2}\left[(1-\delta_{0,n})L_{n-1}\left(\frac{q^2\ell_B^2}{2}\right) + (1+\delta_{0,n})L_n\left(\frac{q^2\ell_B^2}{2}\right)\right]e^{-q^2\ell_B^2/4}.$$

Because we merely focus on the lowest LL $n=0$, the projective Coulomb interaction (2.6) can be reduced to the familiar form[①]

$$H_{\text{int}} = \frac{1}{2}\sum_{\boldsymbol{q}} \frac{2\pi e^2}{\varepsilon|\boldsymbol{q}|}\rho(-\boldsymbol{q})\rho(\boldsymbol{q}). \tag{2.7}$$

where we neglect the tilde symbol and **from now on, we will erase all the background of massless Dirac fermions and form a notion of multi-component non-relativistic particle instead**.

2.2 Introduction of Chern-Simons Fields and K-matrix

The second quantized Hamiltonian of graphene in strong magnetic fields thus takes the form of (for convenience of the following computation of electromagnetic response, apart from the external magnetic field $\boldsymbol{A}$ applied, we also write down the probing pseudo-magnetic field $\boldsymbol{A'}$ explicitly, which results from the symmetrical strained graphene and thus *alters its direction* for different valley index)

$$\begin{aligned} H = &\sum_{\alpha}\int \mathrm{d}^3x\,(\psi_e)^\dagger_\alpha(x)\frac{1}{2m}\left(-i\nabla + e\boldsymbol{A} + e\boldsymbol{A'}^{\alpha}\right)^2(\psi_e)_\alpha(x) \\ &+ \frac{1}{2}\sum_{\alpha\beta}\int \mathrm{d}^3x\,\mathrm{d}^3x'\,\delta(\hat{\rho}_e)_\alpha(x)v_{\alpha\beta}(|\boldsymbol{x}-\boldsymbol{x'}|)\delta(\hat{\rho}_e)_\beta(x'), \end{aligned} \tag{2.8}$$

where

$$\boldsymbol{A'}^{\alpha} = \begin{cases} +\boldsymbol{A'}, & \alpha = \uparrow, \\ -\boldsymbol{A'}, & \alpha = \downarrow, \end{cases}$$

the fluctuation of charge density $\delta(\hat{\psi_e})(x)_a \equiv (\psi_e)^\dagger_\alpha(x)(\psi_e)_\alpha(x) - (\bar{\rho}_e)_\alpha(x)$, and the Coulomb interaction $v(|r|) = \frac{e^2}{\varepsilon|r|}$.

Similar to the situation in HLR, we take the *singular unitary transformation* $(\psi_e)_\alpha \mapsto \psi_\alpha \equiv U_\alpha(\psi_e)_\alpha$ to transfer our strongly-correlated system to an *equivalent*[②] one but easy

[①]The zero Laguerre polynomial $L_0(z) = 0$ for arbitrary z.

[②]By "equivalent", we mean that a physical evaluation in path integral bridge these two systems, cf. appendix A of [20] for details.

to handle with. And in light of the increase of freedom of our field operator (due to valley degeneracy), the unitary operator should be generalized to

$$U_\alpha \equiv \exp\left[i\mathcal{K}^{\alpha\beta}\int \mathrm{d}\boldsymbol{r'}\arg(\boldsymbol{r}-\boldsymbol{r'})\rho_\beta(\boldsymbol{r'})\right] \tag{2.9}$$

in our situation, where the function $\arg(\boldsymbol{r}-\boldsymbol{r'}) \equiv \arctan\frac{y-y'}{x-x'}$ and Einstein's summation rule of repeated greek indices $\alpha,\beta=\uparrow,\downarrow$ is implemented. The general form of $\mathcal{K}$-matrix introduced by Wen and Zee in [52] takes as [31]

$$\mathcal{K}^{\alpha\beta} = \begin{pmatrix} 2k_1 & m \\ m & 2k_2 \end{pmatrix} \tag{2.10}$$

with all k_1, k_2 and m integers because the proof of equivalence in [20] can be safely generalized to fermionic Chern-Simons theory for more freedoms. However, due to the valley symmetry of graphene, every element of $\mathcal{K}$-matrix should be *even* for undistinguishability of fermions. And we do provide one proof in appendix A with the method introduced by Rajaraman in [53] through consideration of the consistent anticommunication relation of canonical quantized fermionic operators.

Defining the vector fields

$$e\boldsymbol{a}^\alpha(\boldsymbol{r}) = \mathcal{K}^{\alpha\beta}\int \mathrm{d}\boldsymbol{r'}\,\nabla\arg(\boldsymbol{r}-\boldsymbol{r'})\rho_\beta(\boldsymbol{r'}) = \mathcal{K}^{\alpha\beta}\int \mathrm{d}\boldsymbol{r'}\,\frac{\varepsilon_{ij}(\boldsymbol{r}_i-\boldsymbol{r}'_j)}{|\boldsymbol{r}-\boldsymbol{r'}|}\rho_\beta(\boldsymbol{r'}), \tag{2.11}$$

then clearly the original Hamiltonian is equivalent to the system with new Chern-Simons gauge fields $\boldsymbol{a}^\alpha$ included[①] [54]

$$\begin{aligned} H = &\sum_\alpha \int \mathrm{d}^3x\,\psi^\dagger_\alpha(x)\frac{1}{2m}\left(-i\nabla + e\boldsymbol{A} + e\boldsymbol{A'}^\alpha - e\boldsymbol{a}^\alpha\right)^2\psi_\alpha(x) \\ &+ \frac{1}{2}\sum_{\alpha\beta}\int \mathrm{d}^3x\,\mathrm{d}^3x'\,\delta\hat{\rho}_\alpha(x)v\alpha\beta(|\boldsymbol{x}-\boldsymbol{x'}|)\delta\hat{\rho}_\beta(x'). \end{aligned} \tag{2.12}$$

So in addition to the external magnetic fields we impose on, each electron at position $\boldsymbol{r}$ is now attached with several other magnetic flux

$$\boldsymbol{B}^\alpha_{\mathrm{CS}} \equiv \nabla\times\boldsymbol{a}^\alpha = -\frac{2\pi}{e}\mathcal{K}^{\alpha\beta}\rho_\beta(\boldsymbol{r}). \tag{2.13}$$

The accurate number of flux attachment, i.e., the element of $\mathcal{K}$-matrix *cannot* be determined in advance, but in light of the *Marginal Fermi-liquid* half-filling FQHE state

① Note that the singular unitary transformation does not change the form of density operator.

studied by [22] in monolayer system, we also believe the existence of Fermi-liquid-like state $\nu = 1/2$ in graphene. In HLR's motivation, **the external magnetic field felt by an arbitrary fermion is accurately eliminated by the Chern-Simons magnetic field**, viz.

$$\boldsymbol{B}^{\alpha}_{\text{eff}} \equiv \boldsymbol{B}_{\text{ext}} + \boldsymbol{B}^{\alpha}_{\text{CS}} = 0. \tag{2.14}$$

But the physical picture is much subtler here since **the attached flux of electrons in one band will certainly influence the electrons in the other band as well, and vice versa**.

Duality of two valley degeneracy of graphene, K and K', guarantees that the number of electrons in each freedom is *the same* (and approximately conserved) $N_1 = N_2 = N/2$ and every electron subjects to the same strength of external magnetic fields, or is bond with the same number of Chern-Simons magnetic flux to compensate the external magnetic fields. Therefore, it's reasonable to have $\nu_\alpha = \frac{(\rho_e)_\alpha S}{BS/\phi_0} = \frac{\nu}{2} = \frac{1}{4}$, as is illustrated in Fig 2.2, which can be realized if the $\mathcal{K}-$matrix is chosen to be *invertible*

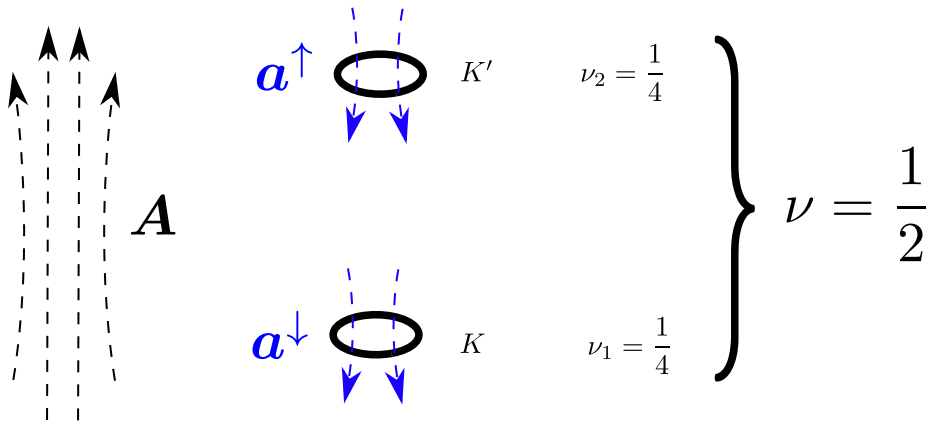

Fig. 2.2 **Compensation of External Magnetic Fields**. Black dashed arrows indicate the external magnetic field $\boldsymbol{B}_{\text{ext}}$, blue dashed arrows indicate opposite $\boldsymbol{B}^{\alpha}_{\text{CS}}$ for each valley, and thick black circles represent electrons. The proportion of number of electrons to the number of magnetic flux, i.e., the Landau filling factors is clearly shown in the figure as well.

$$\mathcal{K}^{\alpha\beta} = \begin{pmatrix} \widetilde{\phi} & \widetilde{\phi} \\ \widetilde{\phi} & \widetilde{\phi} \end{pmatrix} \tag{2.15}$$

with $\widetilde{\phi} = 2$. And all the following computation bases on this assuming matrix.

2.3 Action of Fermionic Chern-Simons Theory

After bringing in the Chern-Simons field in $\nu = 1/2$ FQHE system, composite fermions subject to *zero* effective magnetic field and are now governed by the new Hamiltonian (2.12) as well as the *constraint conditions* (2.13) and (2.14), which, are actually the dynamical equation of Chern-Simons field $\boldsymbol{a}^{\alpha}$. And it is because of our choice of *invertible* $\mathcal{K}-$matrix that leads to the degeneracy of one of the Chern-Simons field since from (2.13) and (2.14) we always have $\boldsymbol{a}^{\uparrow} \equiv \boldsymbol{a}^{\downarrow}$. And from now on we will omit the valley index of Chern-Simons field, simply writing it as $\boldsymbol{a}$ instead.

Working in *Coulomb gauge*, i.e., $\nabla \cdot \boldsymbol{a} = \nabla \cdot \boldsymbol{A} = \nabla \cdot \boldsymbol{A'}^{\alpha} = 0$, then $a_{||}(p) = A_{||}(p) = A'^{\alpha}_{||}(p) = 0$ if we decompose them into *transverse* and *longtitudinal* components (write in momentum space)[①]

$$a_i(p) \equiv \frac{p_i}{|\boldsymbol{p}|} a_{||}(p) + \frac{\varepsilon_{ij} p^j}{|\boldsymbol{p}|} a_{\perp}(p). \tag{2.16}$$

Certainly gauge fixing could also be done *after* writing down the action below, and the standard Fadeev-Popov method in high energy physics is introduced to accomplish this, cf. [55] for details.

For the future unified treatment of Gaussian fluctuation, it is better to recover the dynamical equation of $\boldsymbol{a}$ back into the action such that in coherent state path integral formalism the partition function can be extended to both fermionic fields and Chern-Simons fields (in imaginary time $t \equiv -i\tau$)

$$\begin{aligned}
\mathcal{Z} &= \int \mathcal{D}(\bar{\psi}_{\uparrow}, \psi_{\uparrow}) \mathcal{D}(\bar{\psi}_{\downarrow}, \psi_{\downarrow})\, e^{-S[\bar{\psi}_{\uparrow}, \psi_{\uparrow}, \bar{\psi}_{\downarrow}, \psi_{\downarrow}]} \\
&= \int \mathcal{D}(\bar{\psi}_{\uparrow}, \psi_{\uparrow}) \mathcal{D}(\bar{\psi}_{\downarrow}, \psi_{\downarrow}) \mathcal{D}a_{\perp} \prod_{\boldsymbol{x},\tau} \delta\left(B_{\text{CS}} + \phi_0 \widetilde{\phi}(\rho^{\uparrow} + \rho^{\downarrow})\right)\, e^{-S[\bar{\psi}_{\uparrow}, \psi_{\uparrow}, \bar{\psi}_{\downarrow}, \psi_{\downarrow}, a_{\perp}]} \\
&= \mathcal{Z}_0 \int \mathcal{D}(\bar{\psi}_{\uparrow}, \psi_{\uparrow}) \mathcal{D}(\bar{\psi}_{\downarrow}, \psi_{\downarrow}) \mathcal{D}a_0 \mathcal{D}a_{\perp} \\
&\qquad \exp\left\{ -\int_0^{\beta} \mathrm{d}\tau \int \mathrm{d}\boldsymbol{x} \left(\frac{\varepsilon^{ij} \partial_i a_j}{\phi_0 \widetilde{\phi}} + \rho_{\uparrow} + \rho_{\downarrow} \right) a_0 - S[\bar{\psi}_{\uparrow}, \psi_{\uparrow}, \bar{\psi}_{\downarrow}, \psi_{\downarrow}, a_{\perp}] \right\} \\
&= \mathcal{Z}_0 \int \mathcal{D}(\bar{\psi}_{\uparrow}, \psi_{\uparrow}) \mathcal{D}(\bar{\psi}_{\downarrow}, \psi_{\downarrow}) \mathcal{D}a_0 \mathcal{D}a_{\perp}
\end{aligned}$$

[①] By Helmholz theorem (or Hodge Decomposition), any arbitrary field can be decomposed by an irrotational field and a solenoidal field. Coulomb gauge equation $\nabla \cdot \boldsymbol{a} = 0$ is equivalent to $a_{||} = 0$, since in momentum space

$$\boldsymbol{p} \cdot \boldsymbol{a} = \frac{p_i p^i}{|\boldsymbol{p}|}_{||} + \frac{\varepsilon_{ij} p^j p^i}{|\boldsymbol{p}|} a_{\perp} = \frac{p_i p^i}{|\boldsymbol{p}|} a_{||} = 0 \implies a_{||} = 0.$$

$$\exp\left\{-S_{\text{CF}}[\bar{\psi},\psi,a_0,a_\perp]-S_{\text{int}}[\bar{\psi},\psi]-S_{\text{CS}}[a_0,a_\perp]\right\}, \tag{2.17}$$

where in the first line we insert a functional version of the integral over Dirac delta function[①]

$$\mathbb{1}\equiv\int\mathcal{D}a_\perp\prod_{\boldsymbol{x},\tau}\delta(\varepsilon^{ij}\partial_i a_j+\phi_0\mathcal{K}^{\alpha\beta}\rho_\beta(\boldsymbol{x},\tau)),$$

in the second line we first extract the common factor $\phi_0\widetilde{\mathcal{K}}$, which gives an irrelevant normalization factor $\mathcal{Z}_0$, then perform a *functional version of Fourier Transformation* of Dirac delta function[②] with the dual function denoted as $a_0(\boldsymbol{x},\tau)$

$$\prod_{\boldsymbol{x},\tau}\delta\left(\frac{\varepsilon^{ij}\partial_i a_j}{\phi_0\widetilde{\phi}}+\rho_\uparrow+\rho_\downarrow\right)\equiv\int\mathcal{D}a_0\,\exp\left(-\int_0^\beta\mathrm{d}\tau\int\mathrm{d}^2x\,a_0\left(\frac{\varepsilon^{ij}\partial_i a_j}{\phi_0\widetilde{\phi}}+\rho_\uparrow+\rho_\downarrow\right)\right),$$

and in the third line we re-arrange terms and divide them into three parts

- the action of composite fermion

$$\begin{aligned}S_{\text{CF}}[\bar{\psi},\psi,a_0,a_\perp]=\sum_\alpha\int_0^\beta\mathrm{d}\tau\int\mathrm{d}^2x\,\bar{\psi}_\alpha\Big[&\partial_\tau+\mu-a_0+\\&\frac{1}{2m}(-i\nabla+e\boldsymbol{A}+e\boldsymbol{A'}^\alpha+e\boldsymbol{a})^2\Big]\psi_\alpha,\end{aligned} \tag{2.18}$$

- the action of interacting composite fermions

$$\begin{aligned}S_{\text{int}}[\bar{\psi},\psi]=\sum_{\alpha\beta}\frac{1}{2}\int_0^\beta\mathrm{d}\tau\,\mathrm{d}\tau'\int\mathrm{d}^2x\,\mathrm{d}^2x'\\(\bar{\psi}_\alpha(\boldsymbol{x})\bar{\psi}_\alpha(\boldsymbol{x})-\bar{\rho}_\alpha)v(\boldsymbol{x}-\boldsymbol{x'})(\bar{\psi}_\beta(\boldsymbol{x'})\psi_\beta(\boldsymbol{x})-\bar{\rho}_\beta),\end{aligned} \tag{2.19}$$

- and the action of Chern-Simons field

$$S_{\text{CS}}[a_0,a_\perp]=\frac{1}{\phi_0\widetilde{\phi}}\int_0^\beta\mathrm{d}\tau\int\mathrm{d}^2x\,a_0\varepsilon^{ij}\partial_i a_j. \tag{2.20}$$

[①]Taking the concrete definition of path integral into account helps understand this identity as infinite multiplication of usual Lebesgue integral over the generalized function space

$$\mathbb{1}=\lim_{N\to\infty}\prod_{k=0}^{N}\int\mathrm{d}a_\perp(x_k)\,\delta(\varepsilon^{ij}\partial_i a_j(x_k)+\phi_0\mathcal{K}^{\alpha\beta}\rho_\beta(x_k,t_k)).$$

[②]The Chern-Simons gauge field we brought in before is just of *two-component*. So this functional Fourier Transformation should be regarded as the *definition* of a_0. We write them together just for convenience.

And by Coulomb gauge we can simplify (2.18) by expanding the parentheses

$$\begin{aligned} S_{\text{CF}} &= \sum_{\alpha} \int_0^{\beta} \mathrm{d}\tau \int \mathrm{d}^2 x\, \bar{\psi}_\alpha \Big[\partial_\tau + \mu - a_0 - \frac{1}{2m}\nabla^2 - \frac{ie}{2m}\nabla\cdot(\boldsymbol{A}+\boldsymbol{A'}^{\alpha}+\boldsymbol{a}) \\ &\quad - \frac{ie}{2m}(\boldsymbol{A}+\boldsymbol{A'}^{\alpha}+\boldsymbol{a})\cdot\nabla + \frac{e^2}{2m}(\boldsymbol{A}+\boldsymbol{A'}^{\alpha}+\boldsymbol{a})^2 \Big]\psi_\alpha \\ &= \sum_{\alpha} \int_0^{\beta} \mathrm{d}\tau \int \mathrm{d}^2 x\, \bar{\psi}_\alpha \Big[\mathcal{G}_0^{-1} + \hat{\chi}_1^{\alpha} + \hat{\chi}_2^{\alpha} \Big]\psi_\alpha, \end{aligned} \tag{2.21}$$

where

$$\hat{\mathcal{G}}_0 = \left(\partial_\tau + \mu - \frac{1}{2m}\nabla^2\right)^{-1}, \quad \hat{\chi}_1^{\alpha} \equiv -a_0 - \frac{ie}{m}(\boldsymbol{A}+\boldsymbol{A'}^{\alpha}+\boldsymbol{a})\cdot\nabla, \quad \hat{\chi}_2^{\alpha} = \frac{e^2}{2m}(\boldsymbol{A}+\boldsymbol{A'}^{\alpha}+\boldsymbol{a})^2.$$

Therefore, the partition function can be obtained if we integrate out all freedoms, which are dominated by the above three parts of actions.

2.4 Mean-field Approximation and Gaussian Fluctuation

In this section, we first derive the effection action of gauge field $a_\mu(\boldsymbol{x})$ as Lopez and Fradkin them did in [20]. Subsequently we will expand the effective action to the second order to obtain the Gaussian fluctuation around the mean-field.

Due to the *quartic* form of Coulomb interaction, an direct integration over fermionic operators to obtain the effective action of Chern-Simons field is not readily possible. In fact, a *Hubbard-Stratonovich Transformation* of density-density channel has to be performed before the integration to reduce the power of fermionic operators. Through introducing an auxiliary bosonic operator and shifting it to eliminate the quartic interaction, we are left with a *quadratic* form of this auxiliary field, which can be integrated out standardly with Gauss integral formula [42, 56-57].

However, since the dynamic equation (2.13) and (2.14) exactly connect Chern-Simons field with fermionic field, this standard procedure can be circumvented by simple substitution of ψ with $\boldsymbol{a}$, giving

$$S_{\text{int}} = \frac{1}{2}\int \mathrm{d}^3x\, \mathrm{d}^3x' \left(\frac{\varepsilon^{ij}\partial_i a_j(\boldsymbol{x})}{2\widetilde{\phi}\phi_0} - \bar{\rho}\right) v(\boldsymbol{x}-\boldsymbol{x'}) \left(\frac{\varepsilon^{k\ell}\partial_k a_\ell(\boldsymbol{x'})}{2\widetilde{\phi}\phi_0} - \bar{\rho}\right). \tag{2.22}$$

Now that the left parts of action in (2.17), i.e. the action of composite fermions (2.21), is of quadratic form, then the effective action of bosonic operators can be obtained by integrating out all fermionic freedoms as following

$$S_{\text{CF-eff}}[a_0, a_\perp] = \sum_{\alpha} \ln\det\left[\hat{\mathcal{G}}_0^{-1} + \hat{\chi}_1^{\alpha} + \hat{\chi}_2^{\alpha}\right] = \sum_{\alpha} \operatorname{tr}\ln\left[\hat{\mathcal{G}}_0^{-1} + \hat{\chi}_1^{\alpha} + \hat{\chi}_2^{\alpha}\right]$$

$$= 2\mathrm{tr}\left(\ln \hat{\mathcal{G}}_0^{-1}\right) + \sum_\alpha \mathrm{tr}\left(\hat{\mathcal{G}}_0 \hat{\chi}_1^\alpha\right) + \sum_\alpha \mathrm{tr}\left(\hat{\mathcal{G}}_0 \hat{\chi}_2^\alpha + \frac{1}{2}\hat{\mathcal{G}}_0 \hat{\chi}_1^\alpha \hat{\mathcal{G}}_0 \hat{\chi}_1^\alpha\right)$$
$$+ \mathcal{O}(|a_0|^3, |\boldsymbol{a}|^3). \tag{2.23}$$

The first term is irrelevant to all bosonic freedoms so can be absorbed in $\mathcal{Z}_0$. The second term also vanishes since we expand around the saddle-point $a_\mu : \bar{a}_\mu \mapsto \bar{a}_\mu + a_\mu$, with $\bar{a}_\mu$ subject to the *mean-field equation* (2.13)

$$\varepsilon^{ij}\partial_i \bar{a}_j^\alpha = -\frac{2\pi}{e}\mathcal{K}^{\alpha\beta}\bar{\rho}_\beta(\boldsymbol{x}), \tag{2.24}$$

which is in conformity with the requirement of a vanishing first variation[①]

$$\left.\frac{\delta S}{\delta a_i}\right|_{\substack{\bar{a}_0=0 \\ \varepsilon^{ij}\partial_i\bar{a}_j=-2\phi_0\widetilde{\phi}\bar{\rho}}} = \frac{\delta S_{\text{CF-eff}}}{\delta a_i} + \frac{\delta S_{\text{int}}}{\delta a_i} + \frac{\delta S_{\text{CS}}}{\delta a_i}$$
$$= -\frac{1}{2}\int \mathrm{d}^3x\,\mathrm{d}^3x'\bar{\rho}v(\boldsymbol{x}-\boldsymbol{x'})\left(\frac{\varepsilon^{k\ell}\partial_k\bar{a}_\ell(\boldsymbol{x'})}{2\widetilde{\phi}\phi_0} - \bar{\rho}\right) = 0.$$

So the first non-trivial term contributing to electromagnetic linear response is the second order expansion of (2.23).

Given the gauge condition (2.16) we chose, it's more convenient to simplify the trace in momentum space instead. So we start with re-expressing the action of composite fermions as following

$$S_{\text{CF}} = \sum_\alpha \sum_{\boldsymbol{q}_1,\omega_n} \sum_{\boldsymbol{q}_2,\omega_m} \bar{\psi}_{\alpha,q_1}\left[(\hat{\mathcal{G}}_0^{-1})_{q_1,q_2} + (\hat{\chi}_1^\alpha)_{q_1,q_2} + (\hat{\chi}_2^\alpha)_{q_1,q_2}\right]\psi_{\alpha,q_2}, \tag{2.25}$$

where[②]

$$(\hat{\mathcal{G}}_0^{-1})_{q_1,q_2} \equiv \mathcal{G}_0^{-1}(\boldsymbol{q}_1, i\omega_n)\delta_{\boldsymbol{q}_1,\boldsymbol{q}_2}\delta_{\omega_n,\omega_m}, \tag{2.26a}$$
$$(\hat{\chi}_1^\alpha)_{q_1,q_2} \equiv -a_0(q_1-q_2) - \frac{e}{m}\left(\boldsymbol{a}+\boldsymbol{A}+\boldsymbol{A'}^\alpha\right)(q_1-q_2)\cdot\boldsymbol{q}_2, \tag{2.26b}$$
$$(\hat{\chi}_2^\alpha)_{q_1,q_2} \equiv \frac{e^2}{2m}\sum_q \left(\boldsymbol{a}+\boldsymbol{A}+\boldsymbol{A'}^\alpha\right)(q+q_1)\cdot\left(\boldsymbol{a}+\boldsymbol{A}+\boldsymbol{A'}^\alpha\right)(-q-q_2). \tag{2.26c}$$

[①]Perturbation must comply with the gauge condition of the Chern-Simons fields. So $a_{||}, A_{||}$ and $A'_{||}$ stay to be zero all the time.

[②]Results here is straight to verify. The notation $(\hat{\mathcal{G}}_0^{-1})_{q_1,q_2}$ in (2.26a), for instance, is a conventional notation representing a matrix element in momentum space [42, 54].

Still integrating out the fermionic operators and expanding around saddle point, the first part of the trace now can be shown as

$$
\begin{aligned}
\operatorname{tr}\left(\hat{\mathcal{G}}_0\hat{\chi}_2^\alpha\right) &= \sum_p (\mathcal{G}_0)_p(\chi_2^\alpha)_{p,p} = \frac{e^2}{2m}\sum_{p,q}(\mathcal{G}_0)_p(\boldsymbol{a}+\boldsymbol{A'}^\alpha)_{p+q}\cdot(\boldsymbol{a}+\boldsymbol{A'}^\alpha)_{-p-q} \\
&= \frac{e^2}{2m}\sum_{p,q}(\mathcal{G}_0)_p\frac{\varepsilon^{ij}(p^i+q^i)}{|\boldsymbol{p}+\boldsymbol{q}|}(a_\perp+A'^\alpha_\perp)_{p+q}\frac{\varepsilon_{ik}(-p^k-q^k)}{|\boldsymbol{p}+\boldsymbol{q}|}(a_\perp+A'^\alpha)_{-p-q} \\
&= \sum_q (a_\perp+A'^\alpha_\perp)_{-q}\left(\frac{e^2}{2m}\sum_p(\mathcal{G}_0)_p\right)(a_\perp+A'^\alpha_\perp)_q \\
&= \sum_q (a_\perp+A'^\alpha_\perp)_{-q}\left(-\frac{e^2 n_e}{2m}\right)(a_\perp+A'^\alpha_\perp)_q,
\end{aligned}
\tag{2.27}
$$

where in the last line we shift the integral variable q by $-p$ and substitute the identity

$$
\begin{aligned}
\sum_{\boldsymbol{p},\omega_n}\mathcal{G}_0(\boldsymbol{p},i\omega_n) &= \lim_{\tau\to 0}\sum_{\boldsymbol{p},\omega_n}e^{-i\omega_n\tau}\mathcal{G}_0(\boldsymbol{p},i\omega_n) = \lim_{\tau\to 0}\sum_{\boldsymbol{p}}\mathcal{G}_0(\boldsymbol{p},\tau) \equiv \lim_{\tau\to 0}\sum_{\boldsymbol{p}}\langle T_\tau\psi(\boldsymbol{p},\tau)\psi^\dagger(\boldsymbol{p},\tau)\rangle \\
&= -\sum_{\boldsymbol{p}}\langle\psi^\dagger(\boldsymbol{p})\psi(\boldsymbol{p})\rangle = -\sum_{\boldsymbol{p}}\hat{\rho}(\boldsymbol{p}) = -n_F(\xi_{\boldsymbol{p}}).
\end{aligned}
$$

The second part of the trace is much more tedious

$$
\begin{aligned}
\operatorname{tr}\left(\frac{1}{2}\hat{\mathcal{G}}_0\hat{\chi}_1^\alpha\hat{\mathcal{G}}_0\hat{\chi}_1^\alpha\right) &= \frac{1}{2}\sum_{p,q}(\mathcal{G}_0)_p(a_0+A'^\alpha_0)_{p,q}(\mathcal{G}_0)_q(a_0+A'^\alpha_0)_{q,p} \\
&+ \frac{1}{2}\sum_{p,q}(\mathcal{G}_0)_p(a_0+A'^\alpha_0)_{p,q}(\mathcal{G}_0)_q\left(\frac{e}{m}(\boldsymbol{a}+\boldsymbol{A'}^\alpha)\cdot\boldsymbol{p}\right)_{q,p} \\
&+ \frac{1}{2}\sum_{p,q}(\mathcal{G}_0)_p\left(\frac{e}{m}(\boldsymbol{a}+\boldsymbol{A'}^\alpha)\cdot\boldsymbol{p}\right)_{p,q}(\mathcal{G}_0)_q(a_0+A'^\alpha_0)_{q,p} \\
&+ \frac{1}{2}\sum_{p,q}(\mathcal{G}_0)_p\left(\frac{e}{m}(\boldsymbol{a}+\boldsymbol{A'}^\alpha)\cdot\boldsymbol{p}\right)_{p,q}(\mathcal{G}_0)_q\left(\frac{e}{m}(\boldsymbol{a}+\boldsymbol{A'}^\alpha)\cdot\boldsymbol{p}\right)_{q,p} \\
&= \frac{1}{2}\sum_{p,q}(a_0+A'^\alpha_0)_{-q}\cdot(\mathcal{G}_0)_p(\mathcal{G}_0)_{p+q}\cdot(a_0+A'^\alpha_0)_q \\
&+ \frac{1}{2}\sum_{p,q}(a_0+A'^\alpha_0)_{-q}\cdot(\mathcal{G}_0)_p(\mathcal{G}_0)_{p+q}\frac{ep_i}{m}\frac{\varepsilon^{ij}q_j}{|\boldsymbol{q}|}\cdot(a_\perp+A'^\alpha_\perp)_q \\
&+ \frac{1}{2}\sum_{p,q}(a_\perp+A'^\alpha_\perp)_{-q}\cdot(\mathcal{G}_0)_p(\mathcal{G}_0)_{q+p}\frac{ep_i}{m}\frac{\varepsilon^{ij}q_j}{|\boldsymbol{q}|}\cdot(a_0+A'^\alpha_0)_q \\
&+ \frac{1}{2}\sum_{p,q}(a_\perp+A'^\alpha_\perp)_{-q}\cdot\frac{\varepsilon^{ij}(-q_j)}{|\boldsymbol{q}|}\frac{ep_i}{m}(\mathcal{G}_0)_p(\mathcal{G}_0)_{p+q}\frac{ep_l}{m}\frac{\varepsilon^{kl}q_l}{|\boldsymbol{q}|}\cdot(a_\perp+A'^\alpha_\perp)_q,
\end{aligned}
\tag{2.28}
$$

where in the second equal sign we shift the variable q to $q\mapsto p+q$ as well.

Therefore, summing up all traces, from (2.23) we find the *polarization tensor* $\Pi^{\mu\nu}$ such that

$$S_{\mathrm{CF}} = \frac{1}{2}\sum_{\alpha=\uparrow,\downarrow}\sum_{\mu,\nu}^{0,1}\sum_{\boldsymbol{q},\omega_n}\left(a_\mu + A'^{\alpha}_{\mu}\right)_{-q}\Pi^{\mu\nu}_{\alpha}\left(a_\mu + A'^{\alpha}_{\mu}\right)_{q}, \tag{2.29}$$

with

$$\Pi^{\mu\nu}_{\uparrow} = \Pi^{\mu\nu}_{\downarrow} \equiv \begin{pmatrix} \sum_p (\mathcal{G}_0)_p(\mathcal{G}_0)_{p+q} & \frac{e\varepsilon^{ij}q_j}{m|\boldsymbol{q}|}\sum_p p_i(\mathcal{G}_0)_p(\mathcal{G}_0)_{p+q} \\ \frac{e\varepsilon^{ij}q_j}{m|\boldsymbol{q}|}\sum_p p_i(\mathcal{G}_0)_p(\mathcal{G}_0)_{p+q} & -\frac{e^2 n_e}{m} + \sum_p \frac{e^2p^2}{m^2}(\mathcal{G}_0)_p(\mathcal{G}_0)_{p+q} \end{pmatrix}, \tag{2.30}$$

which coincides with the celebrated results of Halperin *et al.* in [22]. The off-diagonal matrix elements of $\Pi^{\mu\nu}$ can be shown vanishing for $(\mathcal{G}_0)_{p+q}(\mathcal{G}_0)_p \sim (\mathcal{G}_0)_p^2$ is even in momentum under long wavelength limit, cf. appendix B. And diagonal matrix element is calculated in details in appendix C in different extreme conditions as well. The result is (for $q \ll q_F$ and $\omega \ll qv_F$)

$$\Pi^{\mu\nu}_{\uparrow,\downarrow}(\boldsymbol{q},\omega) = \begin{pmatrix} \frac{m}{2\pi} + \mathcal{O}(q^2) & \mathcal{O}(q^2) \\ \mathcal{O}(q^2) & -\frac{q^2}{12\pi m} + i\frac{2n_e\omega}{k_F q} + \mathcal{O}(q^3) \end{pmatrix}. \tag{2.31}$$

To avoid loss of generality, one can also invoke the *Kallen Lehmann spectrum decomposition theorem* [55, 58] to expand the Green function in basis of Landau wave function and express the polarization tensor by lengthy infinite series, as is done by Lopez and Fradkin in [20]. In their paper, they factorize the the polarization tensor into three scalar components, $\Pi^0_\alpha, \Pi^1_\alpha, \Pi^2_\alpha$ for the transversity

$$\partial^x_\mu \Pi^{\mu\nu}_\alpha(x,y) = 0, \tag{2.32}$$

results from gauge invariance of the effective action [59], reading ($i, j = 1, 2$ represent x, y component)

$$\Pi^{00}_\alpha(\boldsymbol{q},\omega) = -\boldsymbol{q}^2\Pi^0_\alpha(\boldsymbol{q},\omega), \tag{2.33a}$$

$$\Pi^{0i}_\alpha(\boldsymbol{q},\omega) = -\omega q^i\Pi^0_\alpha(\boldsymbol{q},\omega) + i\varepsilon^{0ij}q_j\Pi^1_\alpha(\boldsymbol{q},\omega), \tag{2.33b}$$

$$\Pi^{i0}_\alpha(\boldsymbol{q},\omega) = -\omega q^i\Pi^0_\alpha(\boldsymbol{q},\omega) - i\varepsilon^{0ij}q_j\Pi^1_\alpha(\boldsymbol{q},\omega), \tag{2.33c}$$

$$\Pi^{ij}_\alpha(\boldsymbol{q},\omega) = -\omega^2\delta^{ij}\Pi^0_\alpha(\boldsymbol{q},\omega) + i\varepsilon^{0ij}\omega\Pi^1_\alpha(\boldsymbol{q},\omega) + (\delta^i j - q^i q^j)\Pi^2_\alpha(\boldsymbol{q},\omega), \tag{2.33d}$$

with each scalar tensor is given in the Appendix B of [20]. We will return to this method on discussion of the discrepancy of our theory to $\mathrm{SU}(2)$ spin unpolarized fermionic Chern-Simons theory with Zeeman terms in the next chapter.

2.5 Electromagnetic Response Tensor

In order to obtain the electromagnetic response tensor

$$K_{\mu\nu}(x,y) := \frac{\delta^2}{\delta A'_\mu(x)\delta A'_\nu(y)} \ln \mathcal{Z}[\boldsymbol{A'}],$$

we need to integrate out the residue freedom of statistical field a_μ in the effective action. Ditto for the Fourier transformation we performed in the previous section to expressed the action of composite fermions in an explicit form (2.29), the same procedure should be applied with other parts of action. We re-express the action of Chern-Simons field[①] as

$$\begin{aligned} S_{\text{CS}} &= \frac{1}{2}\sum_{\boldsymbol{q},\omega_n} a_0(-\boldsymbol{q},-i\omega_n)\varepsilon^{ij}(-iq_i)\frac{\varepsilon_{jk}q^k}{|\boldsymbol{q}|}a_\perp(\boldsymbol{q},i\omega_n) \\ &\quad + a_\perp(-\boldsymbol{q},-i\omega_n)\varepsilon^{ij}iq_j\frac{\varepsilon_{jk}q^k}{|\boldsymbol{q}|}a_0(\boldsymbol{q},i\omega_n) \\ &= \frac{1}{2}\sum_{\boldsymbol{q},\omega_n} a_0(-\boldsymbol{q},-i\omega_n)\cdot iq\cdot a_\perp(\boldsymbol{q},i\omega_n) + a_\perp(-\boldsymbol{q},-i\omega_n)\cdot(-iq)\cdot a_0(\boldsymbol{q},i\omega_n) \end{aligned} \tag{2.34}$$

and the action of Coulomb interaction[②] as

$$\begin{aligned} S_{\text{int}} &= \frac{1}{2(\widetilde{\phi}\phi_0)^2}\sum_{\boldsymbol{q},\omega_n}\varepsilon^{ij}(-i(-q_i))a_j(-\boldsymbol{q},-i\omega_n)v(\boldsymbol{q},i\omega_n)\varepsilon^{kl}(-iq_k)a_l(\boldsymbol{q},i\omega_n) \\ &= \frac{1}{2(\widetilde{\phi}\phi_0)^2}\sum_{\boldsymbol{q},\omega_n} a_\perp(-\boldsymbol{q},-i\omega_n)\varepsilon^{ij}(-i(-q_i))\frac{\varepsilon_{jk}(-q^k)}{|\boldsymbol{q}|}\varepsilon^{lm}(-iq_l)\frac{\varepsilon_{mn}q^n}{|\boldsymbol{q}|}a_\perp(\boldsymbol{q},i\omega_n) \\ &= \frac{1}{2}\sum_{\boldsymbol{q},\omega_n} a_\perp(-\boldsymbol{q},-i\omega_n)\cdot\left(-\frac{q^2v(q)}{(\widetilde{\phi}\phi_0)^2}\right)\cdot a_\perp(\boldsymbol{q},i\omega_n). \end{aligned} \tag{2.35}$$

which, in addition to (2.29), contributes to the complete effective action of both stimulant magnetic field A'^{α}_{μ} and Chern-Simons field a_μ

$$S_{\text{eff}}[a_\mu, A'^{\alpha}_{\mu}] = \frac{1}{2}\sum_{\mu,\nu}^{0,1}\sum_{\boldsymbol{q},\omega_n}\left(a_\mu + A'^{\uparrow}_{\mu}\right)_{-q}\Pi^{\mu\nu}_{\uparrow}\left(a_\mu + A'^{\uparrow}_{\mu}\right)_{q}$$

---

①The Fourier transformed Chern-Simons action is symmetrically splitted

$$\begin{aligned} \int \mathrm{d}\tau \int \mathrm{d}^x\, a_0\varepsilon^{ij}\partial_i a_j &= \sum_{\boldsymbol{p},\omega_n}\sum_{\boldsymbol{q},\zeta_n} a_0(\boldsymbol{p},i\omega_n)\varepsilon^{ij}p_i a_j(\boldsymbol{q},i\zeta_n)\delta(\omega_n+\zeta_n)\delta(\boldsymbol{p}+\boldsymbol{q}) \\ &= \frac{1}{2}\sum_{\boldsymbol{q},\zeta_n} a_0(-\boldsymbol{q},-i\zeta_n)\varepsilon^{ij}(-iq_i)a_j(\boldsymbol{q},i\zeta_n) + \frac{1}{2}\sum_{\boldsymbol{p},\omega_n} a_0(\boldsymbol{p},i\omega_n)\varepsilon^{ij}ip_i a_j(-\boldsymbol{p},-i\omega_n), \end{aligned}$$

and the transverse component decomposition of $a_i(q)$ is utilized.

②One should be aware that the sum over momentum has no term of $\boldsymbol{q} = \boldsymbol{0}$ for the compensation brought by positive charged background [60].

$$+\left(a_\mu + A'^{\downarrow}_\mu\right)_{-q} \Pi^{\mu\nu}_{\downarrow} \left(a_\mu + A'^{\downarrow}_\mu\right)_q + (a_\mu)_{-q} C^{\mu\nu} (a_\nu)_q, \tag{2.36}$$

where

$$C^{\mu\nu} = \begin{pmatrix} 0 & \dfrac{iq}{\phi_0\widetilde{\phi}} \\ \dfrac{iq}{\phi_0\widetilde{\phi}} & -\dfrac{q^2 v(q)}{(\phi_0\widetilde{\phi})^2} \end{pmatrix}. \tag{2.37}$$

If the fluctuation of electromagnetic field is given by the opposite psuedomagnetic field we introduced in chapter one that $A'^{\uparrow}_\mu = -A'^{\downarrow}_\mu = A'_\mu$, then (2.36) reduces to

$$\begin{aligned} S_{\text{eff}}[a_\mu, A'^{\alpha}_\mu] = \frac{1}{2}\sum_{\mu,\nu}^{0,1}\sum_{\boldsymbol{q},\omega_n} (a_\mu)_{-p}\left(\Pi^{\mu\nu}_{\uparrow} + \Pi^{\mu\nu}_{\downarrow} + C^{\mu\nu}\right)(a_\nu)_p + (a_\mu)_{-p}(\Pi^{\mu\nu}_{\uparrow} - \Pi^{\mu\nu}_{\downarrow})(A'_\nu)_p \\ + (A'_\mu)_{-p}(\Pi^{\mu\nu}_{\uparrow} - \Pi^{\mu\nu}_{\downarrow})(a_\nu)_p + (A'_\mu)_{-p}(\Pi^{\mu\nu}_{\uparrow} + \Pi^{\mu\nu}_{\downarrow})(A'_\nu)_p. \end{aligned} \tag{2.38}$$

After applying the Gaussian integral formula for boson fields①, we end up with

$$\begin{aligned} S_{\text{eff}}[A'_\mu] &= \frac{1}{2}\sum_{\mu,\nu}^{0,1}\sum_{\boldsymbol{q},\omega_n} -\left((\Pi^{\mu\nu}_{\uparrow} - \Pi^{\mu\nu}_{\downarrow})(A'_\mu)_{-p}\right)^{\dagger}\left(\Pi^{\mu\nu}_{\uparrow} + \Pi^{\mu\nu}_{\downarrow} + C^{\mu\nu}\right)^{-1} \\ &\quad \times \left((\Pi^{\mu\nu}_{\uparrow} - \Pi^{\mu\nu}_{\downarrow})(A'_\mu)_{-p}\right) + (A'_\mu)_{-p}(\Pi^{\mu\nu}_{\uparrow} + \Pi^{\mu\nu}_{\downarrow})(A'_\nu)_p \\ &= \frac{1}{2}\sum_{\mu,\nu}^{0,1}\sum_{\boldsymbol{q},\omega_n} \boldsymbol{A'}^{\dagger}\boldsymbol{K}\boldsymbol{A'}, \end{aligned} \tag{2.39}$$

where

$$\boldsymbol{K} \equiv -(\boldsymbol{\Pi}_{\uparrow} - \boldsymbol{\Pi}_{\downarrow})(\boldsymbol{\Pi}_{\uparrow} + \boldsymbol{\Pi}_{\downarrow} + \boldsymbol{C})^{-1}(\boldsymbol{\Pi}_{\uparrow} - \boldsymbol{\Pi}_{\downarrow}) + (\boldsymbol{\Pi}_{\uparrow} + \boldsymbol{\Pi}_{\downarrow}) = 2\boldsymbol{\Pi} \tag{2.40}$$

for $\boldsymbol{\Pi}_{\uparrow}$ has no difference with $\boldsymbol{\Pi}_{\downarrow}$ in our situation, as is seen in (2.30).

The electromagnetic response tensor (2.40) looks counter-intuitive at the first glimpse, because through computation in appendix C the polarization tensor $\boldsymbol{\Pi}$ tends to be *diagnoal* at the long wave-length limit (2.31), revealing **the Hall conductance to be *vanishing***

$$\sigma_{xy} \equiv \lim_{\omega\to 0}\lim_{\boldsymbol{q}\to 0}\frac{i}{q}K_{01}(\boldsymbol{q},\omega) = 0 \tag{2.41}$$

for the momentum order of $K_{01}(\boldsymbol{q},\omega)$ is no less than two.

① $$\int \mathcal{D}\varphi\, e^{-\frac{1}{2}\varphi^{\dagger}a\varphi + \frac{1}{2}\varphi^{\dagger}b + \frac{1}{2}b^{\dagger}\varphi} = (2\pi)^{N/2}\det a^{-1/2}\, e^{-\frac{1}{2}b^{\dagger}a^{-1}b},$$

However, this is not a problem because the opposite pseudomagnetic field we impose alters the sign of coupling between kinetic terms and magnetic vector potential in Hamiltonian. In fact, if we exert the magnetic field fluctuation pointing the same direction to each valley as usual, (2.40) becomes

$$\boldsymbol{K} \equiv -(\boldsymbol{\Pi}_\uparrow + \boldsymbol{\Pi}_\downarrow)(\boldsymbol{\Pi}_\uparrow + \boldsymbol{\Pi}_\downarrow + \boldsymbol{C})^{-1}(\boldsymbol{\Pi}_\uparrow + \boldsymbol{\Pi}_\downarrow) + (\boldsymbol{\Pi}_\uparrow + \boldsymbol{\Pi}_\downarrow),$$

or equivalently[①] ($\boldsymbol{\Pi}^\uparrow = \boldsymbol{\Pi}^\downarrow$ still holds)

$$\boldsymbol{K}^{-1} = (2\boldsymbol{\Pi})^{-1} + \boldsymbol{C}^{-1}, \tag{2.42}$$

in which the Hall conductance correctly reappears, giving

$$\sigma_{xy} \equiv \lim_{\omega\to 0}\lim_{\boldsymbol{q}\to 0}\frac{i}{q}K_{01}(\boldsymbol{q},\omega) = \lim_{\omega\to 0}\lim_{\boldsymbol{q}\to 0}\frac{i}{q}\frac{iq}{\phi_0\widetilde{\phi}} = \frac{e^2}{2\pi\hbar}\nu \tag{2.43}$$

with $\nu = 1/\widetilde{\phi}$.

However, what really counts in our situation is never the quantity of Hall conductance but the behavior of longitudinal one

$$\sigma_{xx}(\boldsymbol{q},\omega) \equiv \frac{\omega}{i|\boldsymbol{q}|^2}K_{00}(\boldsymbol{q},\omega) \tag{2.44}$$

because singularities of K_{00} characterize the gapless excitation spectrum (cf. appendix C), determine the property of marginal Fermi liquid [23] and enable HLR theory acknowledged by the theoretical community. One interesting observation is that, whatever the magnetic field fluctuation one exerts, we always obtain the *doubled* longitudinal conductance in comparison with the results in [22]. This quantitive discrepancy can be verified in surface acoustic wave (SAW) experiments of graphene [8].

Although the off-diagonal elements are absent in our electromagnetic response tensor, this discrepancy, in addition to a quantitive relation of diagonal elements with HLR's results, will not influence the property of Chern-Simons fields's Green function[②]

$$\mathcal{D} = (\boldsymbol{\Pi} + \boldsymbol{C})^{-1}. \tag{2.45}$$

Hence all results in HLR's theory [22], from the asymtotic expression of low-temperature entropy and self-energy of quasiparticles to the model of modified RPA (to accommo-

[①] It's easy to verify that $\boldsymbol{K}^{-1}\boldsymbol{K} = \boldsymbol{K}\boldsymbol{K}^{-1} = \mathbb{1}$.

[②] Propagator of Chern-Simons field can be obtained by integrating out all magnetic vector potentials in the action.

date the infrared divergence behavior of effective mass), are also possessed in our system. So we conclude that **the Lowest half-filling LL of graphene with equal flux attachment to each freedom, is a marginal Fermi-liquid-like compressible state**.

Chapter 3 Discussions And Outlooks

3.1 Remarks on Non-relativistic Fermionic Theory

We have justified that the Hamiltonian projected to the lowest LL, both free parts and interactive parts, is identical to the Hamiltonian encountered in systems with a non-relativistic parabolic dispersion relation at the beginning of chapter two. Since valley degeneracy is the only additional structure, our demonstration is certainly successful in construction of Jain's trial sequences and functions.

But apparently there are still some drawbacks of our effective field theory. If we consider FQHE state with Landau filling factor more than one, then the involvement of other LLs will first bring back the two decoupled sublattice degeneracy and change the Chern-Simons gauge group from $\mathrm{SU}(2)$ to a new one like $\mathrm{SU}(4)$, $\mathrm{SU}(2)^{\otimes 2}$, or $\mathrm{U}(1)^{\otimes 4}$, then break down the simple form of Coulomb interaction (2.5) but leave with the complicated projective interaction (2.4). Also, numerical studying of *LL mixing* on FQHE in graphene [61-62] reveals that LL mixing starts to take effect beyond the zeroth LL, strongly breaking particle-hole symmetry and producing qualitatively different results compared to the lowest Landau level. When it comes to particle-hole symmetry, one may discern the different origin for non-relativistic or relativistic systems. For the former, it is only an emergent symmetry of the lowest LL projective Hamiltonian (inheriting from sublattice degeneracy), while for the latter, it is an exact symmetry of the unprojective Hamiltonian, which even won't be influenced if LL mixing is taken into account.

3.2 Similarities and Discrepancies with Spin Unpolarized Fermionic Chern-Simons Theory

One may impugn our theory that we has nothing different from the well-developed spin polarized or unpolarized fermionic Chern-Simons theory [31-32] for both theories share a similar mathematical structure except for the Zeeman splitting term[①] (after sin-

[①]Zeeman energy alters for each spin freedoms so we add an superscript α on external magnetic field $\boldsymbol{A}$.

gular gauge transformation)

$$H_{\text{Zeeman}} = \sum_{\alpha} \int \mathrm{d}^3x\, \psi_\alpha^\dagger \left(\frac{1}{2}\mu_B \nabla \times (\boldsymbol{A}^\alpha + \boldsymbol{A}'^\alpha + \boldsymbol{a}) \right) \psi_\alpha. \tag{3.1}$$

However, **it is the exactly existence of Zeeman term that distinguishes our theory to theirs**. Besides the opposite sign brought by the pseudomagnetic magnetic field fluctuation, uniformity of $\mathbf{\Pi}_\uparrow$ and $\mathbf{\Pi}_\downarrow$ also plays an non-ignorable role in leading the vanishing Hall conductance in (2.41), which, if we trace back to the source, stems from the Hamiltonian we give at the very beginning.

This additional Zeeman term (3.1), if added, gives rise to a discrepancy on definition of $\hat{\chi}_1^\alpha$ in (2.26b) and thus influences $\mathbf{\Pi}_\uparrow$ and $\mathbf{\Pi}_\downarrow$ at long wave-length limit [31]

$$\Pi^0_{\uparrow,\downarrow}(\boldsymbol{q},\omega) = -\frac{e^2 p}{2\pi} \frac{\omega_c^2}{\omega^2 - \omega_c^2} =: \Pi^0, \tag{3.2a}$$

$$\Pi^1_{\uparrow,\downarrow}(\boldsymbol{q},\omega) = \omega_c \Pi_0 =: \Pi^1, \tag{3.2b}$$

$$\Pi^2_{\uparrow}(\boldsymbol{q},\omega) = -\frac{e^2}{4\pi m^*}\omega_c^2 \left[\frac{3}{\omega^2 - \omega_c^2} - \frac{4}{\omega^2 - 4\omega_c^2} \right] p \left(p - \frac{g m^*}{2 m_e} \right), \tag{3.2c}$$

$$\Pi^2_{\downarrow}(\boldsymbol{q},\omega) = -\frac{e^2}{4\pi m^*}\omega_c^2 \left[\frac{3}{\omega^2 - \omega_c^2} - \frac{4}{\omega^2 - 4\omega_c^2} \right] p \left(p + \frac{g m^*}{2 m_e} \right), \tag{3.2d}$$

where ω_c is the cyclotron frequency

$$\omega_c = \frac{\phi_0 n_e \widetilde{\phi}}{m}, \tag{3.3}$$

p is an integer tending to be infinity[①] and all $\Pi^0_\alpha, \Pi^1_\alpha$ and Π^2_α are introduced in (2.33) before.

Nevertheless, noting that only *real spins* of electrons and external magnetic fields could couple with each other and contribute a Zeeman splitting term, in our situation where components of spinor ψ_α represent valley pseudospins instead, no Zeeman effect should be taken into account and thus the property of $\mathbf{\Pi}_\uparrow \equiv \mathbf{\Pi}_\downarrow$ makes our theory distinct from other spin polarized or non-polarized fermionic Chern-Simons theory.

3.3 Outlooks

In light of the impressive effective model proposed by D. T. Son in [63], where the composite fermion in hall-filled LL with exact particle-hole symmetry is massless Dirac

[①] Half-filling state can be mathematically understood as the limit of FQHE states $\nu = \frac{p}{2p+1}$ with $p \to \infty$.

fermion, characterized by a Berry phase of π around the Fermi circle, and the flaws we disclosed at the beginning of this chapter, a general theory of Fermionic Chern-Simons theory for Dirac particles should also been studied, and Fräßdorf accomplish this in his latest paper [64] with the inspiration of Lopez and Fradkin. It's plausible to expect consistent results between ours and his. So any quantitive and falsfiasible prediction on electromagnetic response or heat response will help in reduction of many theoretical models on FQHE.

Enlargement of the Chern-Simons gauge groups also brings in new diversities for sublattice, valley, and mixed polarizations [32], by which multi-layer Jain's series can be well classified. So a natural question is raised that how to determine physical states from the highly degenerate states with thousands patterns of flux attachment. The answer may not be clear in Fermionic Chern-Simons theory for the constraint condition, for example, canceling out the external magnetic field, is much less than the independent elements of $\mathcal{K}$-matrix.

Appendix A Proof of the General Form of K-matrix

In this appendix, we will give a simple derivation about the general form of $\mathcal{K}$-matrix for multi-layer Fermionic Chern-Simons theory. Lopez and Frakdin has promoted their proof of path integral formalism to double layer case in [30] to attribute the form of $\mathcal{K}$-matrix as topological quantities. But here we will follow the approach of Rajaraman in [53] to obtain the same result in a quicker way.

All fermionic field operators, no matter transformed or not, obey the equal-time anticommunication relations

$$\{\psi_\alpha(\boldsymbol{x}), \psi_\beta(\boldsymbol{x'})\} = \{\psi_\alpha^\dagger(\boldsymbol{x}), \psi_\beta^\dagger(\boldsymbol{x'})\} = 0, \quad \{\psi_\alpha^\dagger(\boldsymbol{x}), \psi_\beta(\boldsymbol{x'})\} = \delta_{\alpha\beta}\delta(\boldsymbol{x}-\boldsymbol{x'}),$$

so for density operator ρ_α we have

$$[\rho_\alpha(\boldsymbol{x}), \psi_\beta(\boldsymbol{x'})] = -\delta_{\alpha\beta}\psi_\beta(\boldsymbol{x'})\delta(\boldsymbol{x}-\boldsymbol{x'}). \tag{A.1}$$

Because of the Pauli exclusion principle, high order of the exponential U_α vanishes for fermionic density operators, thus

$$\begin{aligned}
U_\alpha\psi_\gamma(\boldsymbol{x''}) &= \exp\left[\mathcal{K}^{\alpha\beta}\int \mathrm{d}\boldsymbol{x'}\arg(\boldsymbol{x}-\boldsymbol{x'})\rho_\beta(\boldsymbol{x'})\right]\psi_\gamma(\boldsymbol{x''}) \\
&= \left(1+\mathcal{K}^{\alpha\beta}\int \mathrm{d}\boldsymbol{x'}\arg(\boldsymbol{x}-\boldsymbol{x'})\rho_\beta(\boldsymbol{x'})\right)\psi_\gamma(\boldsymbol{x''}) \\
&= \psi_\gamma(\boldsymbol{x''}) + \mathcal{K}^{\alpha\beta}\int \mathrm{d}\boldsymbol{x'}\arg(\boldsymbol{x}-\boldsymbol{x'})\left(\psi_\gamma(\boldsymbol{x''})\rho_\beta(\boldsymbol{x'}) - \delta_{\beta\gamma}\delta(\boldsymbol{x}-\boldsymbol{x'})\psi_\beta(\boldsymbol{x'})\right) \\
&= \psi_\gamma(\boldsymbol{x''})\exp\left[\mathcal{K}^{\alpha\beta}\left(\int \mathrm{d}\boldsymbol{x'}\arg(\boldsymbol{x}-\boldsymbol{x'})\rho_\beta(\boldsymbol{x'}) + \delta_{\alpha\gamma}\arg(\boldsymbol{x}-\boldsymbol{x''})\right)\right] \\
&= (z-z'')^{\mathcal{K}^{\alpha\gamma}}\psi_\gamma(\boldsymbol{x''})U_\alpha,
\end{aligned} \tag{A.2}$$

and

$$\psi_\gamma^\dagger(\boldsymbol{x''})U_\alpha = (z-z'')^{\mathcal{K}^{\alpha\gamma}}U_\alpha\psi_\gamma^\dagger(\boldsymbol{x''}). \tag{A.3}$$

Utilizing the above identities one can verify that

$$\psi_\alpha(\boldsymbol{x})\psi_\beta(\boldsymbol{x'}) = (-1)^{\mathcal{K}^{\alpha\beta}+1}(z-z')^{\mathcal{K}^{\alpha\beta}-\mathcal{K}^{\beta\alpha}}\psi_\beta(\boldsymbol{x'})\psi_\alpha(\boldsymbol{x}). \tag{A.4}$$

The explicit $(z-z')$ dependence in (A.4) drops out only if the $\mathcal{K}$-matrix chosen to be *symmetric*. Fermions in the same freedom must comply with the anticommunication

relation (A.1) so all diagonal matrix element $\mathcal{K}^{\alpha\alpha}$ must be *even*. As for off-diagonal elements $\mathcal{K}^{\alpha\beta}$ with $\alpha \neq \beta$, whether they are taken to be odd or even depends on communication relation or anticommunication relation the inter-layer fermions comply with.

Lopez and Fradkin derive the general form of (2.10) in [30] under the assumption of distinguishability of fermions between distinct layers. But here by *valley duality* of graphene one should not take fermions as distinguishable any more. Thus every element of $\mathcal{K}$-matrix is set to be even in our case.

Appendix B Validy of Diagonal Polarization Tensor at Long Wave-length Limit

In Halperin *et al.*'s paper [22], the polarization tensor $\Pi_{\uparrow,\downarrow}$ is manifestly diagnalized. To see is, we will check that $\Pi^{01}_{\uparrow,\downarrow}$ and $\Pi^{10}_{\uparrow,\downarrow}$ tend to zero more quickly under long wave-length approximation than the corresponding matrix element, Chern-Simons term $\pm iq/\widetilde{\phi}\phi_0$ in $C_{\mu\nu}$ does. More specifically, we expect the asymtotic property

$$\Pi^{01}_{\uparrow,\downarrow}(\boldsymbol{q}, i\omega_m) = \Pi^{10}_{\uparrow,\downarrow}(\boldsymbol{q}, i\omega_m) = \sum_{p_n} \int \mathrm{d}p^2 \, \frac{e\boldsymbol{p}}{2m} \frac{1}{ip_n - \xi_{\boldsymbol{p}}} \frac{1}{ip_n + i\omega_m - \xi_{\boldsymbol{p}+\boldsymbol{q}}} \sim \mathcal{O}(q^\alpha) \tag{B.1}$$

Holds for $\alpha > 1$. In fact, noting that

$$\begin{aligned}\frac{1}{ip_n + i\omega_m - \xi_{\boldsymbol{p}+\boldsymbol{q}}} &\sim \frac{1}{ip_n + i\omega_m - \boldsymbol{p}^2/2m - |\boldsymbol{p}||\boldsymbol{q}|/m\cos\theta + \mathcal{O}(q^2)} \\ &\sim \frac{1}{ip_n + i\omega_m - \boldsymbol{p}^2/2m} + \frac{|\boldsymbol{p}||\boldsymbol{q}|/m\cos\theta}{(ip_n + i\omega_m - \boldsymbol{p}^2/2m)^2} + \mathcal{O}(q^2),\end{aligned}$$

we conclude

$$\Pi^{01}_{\uparrow,\downarrow} = \Pi^{10}_{\uparrow,\downarrow} \sim \mathcal{O}(q^2).$$

So the off-diagonal element of $\boldsymbol{\Pi}_{\uparrow,\downarrow}$ can be dropped out under long wave-length limit for the integrand of the first term is odd in momentum and the integral of angular variable in the second term always give zero.

Appendix C Evaluation of Polarization Tensor and Excitation Spectrum under Long Wave-length Limit

In this section, we will compute in detail the matrix elements of the polarization tensor (2.38). Since FQHE experiments are performed under extreme low temperature, we direct integral in zero temperature limit and return to *real-time* formalism[①].

As is proven in appendix B, off-diagonal element of $\mathbf{\Pi}$ can be neglected at long wave length limit. So we start from considering the integral

$$\Pi_{00}(\boldsymbol{q},\omega) = i\int \frac{\mathrm{d}E\,\mathrm{d}^2p}{(2\pi)^3}\frac{1}{E-\xi_{\boldsymbol{p}}+i\delta_{\boldsymbol{p}}}\frac{1}{E+\omega-\xi_{\boldsymbol{p}+\boldsymbol{q}}+i\delta_{\boldsymbol{p}+\boldsymbol{q}}}.$$

Obviously only when two singularities are placed on the opposite sides of half plane can we obtain a non-vanishing value (otherwise we can always choose the semi-circle enclosing no singularity as the integral contour). There are two cases:

$$E_1 = \xi_{\boldsymbol{p}} + i\delta, \quad \xi_{\boldsymbol{p}} < 0; \quad E_2 = \xi_{\boldsymbol{p}+\boldsymbol{q}} - \omega - i\delta, \quad \xi_{\boldsymbol{p}+\boldsymbol{q}} > 0;$$
$$E_1 = \xi_{\boldsymbol{p}} - i\delta, \quad \xi_{\boldsymbol{p}} > 0; \quad E_2' = \xi_{\boldsymbol{p}+\boldsymbol{q}} - \omega + i\delta, \quad \xi_{\boldsymbol{p}+\boldsymbol{q}} < 0.$$

Hence by Cauchy theorem, we have

$$\begin{aligned}\Pi_{00}(\boldsymbol{q},\omega) &= i\int \frac{\mathrm{d}^2p}{(2\pi)^3}(2\pi i)\Big(\mathrm{Res}(E_1) + (-1)\mathrm{Res}(E_1')\Big)\\ &= \int_{\xi_{\boldsymbol{p}}<0,\xi_{\boldsymbol{p}+\boldsymbol{q}}>0}\frac{1}{\xi_{\boldsymbol{p}}+\omega-\xi_{\boldsymbol{p}+\boldsymbol{q}}+i\delta}\frac{\mathrm{d}^2p}{(2\pi)^2}\\ &\quad - \int_{\xi_{\boldsymbol{p}}>0,\xi_{\boldsymbol{p}+\boldsymbol{q}}<0}\frac{1}{\xi_{\boldsymbol{p}}+\omega-\xi_{\boldsymbol{p}+\boldsymbol{q}}-i\delta}\frac{\mathrm{d}^2p}{(2\pi)^2},\end{aligned} \tag{C.1}$$

where for the first case we choose the lower semi-circle while for the second case we choose the upper one.

C.1 Static Limit $\omega = 0$

We first consider the density-density component of response function at zero fre-

[①]Remember to add appropriate times of i when transferring self-energy from imaginary time to real time for the difference on definition of Green function on both formalisms

$$\mathcal{G}(p,\tau;p',\tau') := -\langle T_\tau a_p(\tau)a_{p'}^\dagger(\tau')\rangle, \quad G(p,t;p',t') = (-i)\langle T a_p(t)a_{p'}^\dagger(t')\rangle.$$

quency $\Pi_{00}(\boldsymbol{q},0)$.

$$\Pi_{00}(\boldsymbol{q},0)=\int_{\xi_{\boldsymbol{p}}<0}\frac{1}{\xi_{\boldsymbol{p}}-\xi_{\boldsymbol{p}+\boldsymbol{q}}+i\delta}\frac{\mathrm{d}^2p}{(2\pi)^2}-\int_{\xi_{\boldsymbol{p}}>0}\frac{1}{\xi_{\boldsymbol{p}}-\xi_{\boldsymbol{p}+\boldsymbol{q}}-i\delta}\frac{\mathrm{d}^2p}{(2\pi)^2}. \tag{C.2}$$

By Sokhotsky-Wiestrass formula[①], Π_{00} can be computed through figuring our the real part and imaginary part separately

$$\Pi_{00}(\boldsymbol{q},0)=\mathcal{R}e\,\Pi_{00}+i\,\mathcal{I}m\,\Pi_{00}.$$

However, clearly imaginary part of Π_{00} vanishes since both integral conditions can be equaly transformed to

$$\begin{aligned}\xi_{\boldsymbol{p}}<0\bigcap\xi_{\boldsymbol{p}+\boldsymbol{q}}>0 &\implies \frac{pq}{m}\cos\theta+\frac{q^2}{2m}>\mu-\frac{p^2}{2m}>0,\\ \xi_{\boldsymbol{p}}>0\bigcap\xi_{\boldsymbol{p}+\boldsymbol{q}}<0 &\implies \frac{pq}{m}\cos\theta+\frac{q^2}{2m}<\mu-\frac{p^2}{2m}<0\end{aligned}$$

so that

$$\begin{aligned}\mathcal{I}m\,\Pi_{00}(\boldsymbol{q},0)=&\int_{\frac{pq}{m}\cos\theta+\frac{q^2}{2m}>0}\frac{\mathrm{d}^2p}{(2\pi)^2}\pi\times\delta\left(\frac{pq}{m}\cos\theta+\frac{q^2}{2m}\right)\\ &-\int_{\frac{pq}{m}\cos\theta+\frac{q^2}{2m}<0}\frac{\mathrm{d}^2p}{(2\pi)^2}\pi\times\delta\left(\frac{pq}{m}\cos\theta+\frac{q^2}{2m}\right)\equiv 0.\end{aligned}$$

As for the real part,

$$\begin{aligned}\mathcal{R}e\,\Pi_{00}(\boldsymbol{q},0)&=\mathcal{P}\int\frac{n_F(\xi_{\boldsymbol{p}})(1-n_F(\xi_{\boldsymbol{p}+\boldsymbol{q}}))}{\xi_{\boldsymbol{p}}-\xi_{\boldsymbol{p}+\boldsymbol{q}}}-\frac{n_F(\xi_{\boldsymbol{p}+\boldsymbol{q}})(1-n_F(\xi_{\boldsymbol{p}}))}{\xi_{\boldsymbol{p}}-\xi_{\boldsymbol{p}+\boldsymbol{q}}}\frac{\mathrm{d}^2p}{(2\pi)^2}\\ &=\int\left(\frac{n_F(\xi_{\boldsymbol{p}})}{\xi_p-\xi_{\boldsymbol{p}+\boldsymbol{q}}}-\frac{n_F(\xi_{\boldsymbol{p}+\boldsymbol{q}})}{\xi_p-\xi_{\boldsymbol{p}+\boldsymbol{q}}}\right)\frac{\mathrm{d}^2p}{(2\pi)^2}\\ &=\int\left(\frac{n_F(\xi_{\boldsymbol{p}})}{\xi_p-\xi_{p+q}}-\frac{n_F(\xi_{\boldsymbol{p}})}{\xi_{p-q}-\xi_p}\right)\frac{\mathrm{d}^2p}{(2\pi)^2}\\ &\equiv\int_{p<p_F}\frac{-1}{\frac{pq}{m}\cos\theta+\frac{q^2}{2m}}-\frac{1}{\frac{q^2}{2m}-\frac{pq}{m}\cos\theta}\frac{\mathrm{d}^2p}{(2\pi)^2}\\ &=\int_{p<p_F}\frac{4m}{q^2-4p^2\cos^2\theta}\frac{\mathrm{d}^2p}{(2\pi)^2},\end{aligned}$$

where in the first line we introduce the Fermion-Dirac distribution $n_F(\xi_{\boldsymbol{p}})\equiv\Theta(\frac{p2}{2m}-\mu)$ to re-express the confinement on integral variables, and in the second line we shift the dummy variable $\boldsymbol{p}$ to $\boldsymbol{p}-\boldsymbol{q}$ to unify the integral domain for convenience.

① $\frac{1}{x\pm i\delta}=\mathcal{P}\frac{1}{x}\mp i\pi\delta(x)$.

Since no constraint is imposed on the angle variable, integration over θ should be done directly, which naturally brings in another confinement $p < \frac{q}{2}$ since we only concern about the real part of the integral. However, in our case fluctuation of Chern-Simons fields is thought to be faint $q \ll p_F$ so the upper limit of momentum should be replaced with $\frac{q}{2}$ such that

$$\mathcal{R}e\,\Pi_{00}(\boldsymbol{q},0) = \frac{m}{\pi^2}\int_{p<\frac{q}{2}} p\,\mathrm{d}p \int_0^{2\pi} \frac{\mathrm{d}\theta}{q^2-4p^2\cos^2\theta} = \frac{2m}{\pi q}\int_{p<\frac{q}{2}} \frac{p\,\mathrm{d}p}{\sqrt{q^2-4p^2}} = \frac{m}{2\pi}. \tag{C.3}$$

Similar procedure is also applied to the transverse response function $\Pi_{11}(\boldsymbol{q},0)$, giving

$$\begin{aligned}
\mathcal{I}m\,\Pi_{11}(\boldsymbol{q},0) &= 0 \\
\mathcal{R}e\,\Pi_{11}(\boldsymbol{q},0) &= \frac{m}{\pi^2}\int_{p<\frac{q}{2}} p\,\mathrm{d}p \int_0^{2\pi} \frac{e^2p^2}{m^2}\frac{\mathrm{d}\theta}{q^2-4p^2\cos^2\theta} \\
&= \frac{2e^2}{\pi m q}\int_{p<\frac{q}{2}} \frac{p^3\,\mathrm{d}p}{\sqrt{q^2-4p^2}} = -\frac{e^2q^2}{12\pi m}.
\end{aligned} \tag{C.4}$$

C.2 Low Frequency Limit $\omega \ll qp_F/m$

In order to finding out the asymptotic behavior of excitation spectrum, it is also necessary to acquire the explicit expression at both small momentum and small frequency. And we will accomplish this in this section.

Re-expressing the confinements on integral domain of (C.1) by Fermi-Dirac distribution as above, we have

$$\Pi_{00} = \int \frac{n_F(\xi_{\boldsymbol{p}})(1-n_F(\xi_{\boldsymbol{p}+\boldsymbol{q}}))}{\omega+\xi_{\boldsymbol{p}}-\xi_{\boldsymbol{p}+\boldsymbol{q}}+i\delta} - \frac{(1-n_F(\xi_{\boldsymbol{p}}))n_F(\xi_{\boldsymbol{p}+\boldsymbol{q}})}{\omega+\xi_{\boldsymbol{p}}-\xi_{\boldsymbol{p}+\boldsymbol{q}}-i\delta}\frac{\mathrm{d}^2p}{(2\pi)^2}. \tag{C.5}$$

This complicated integration will again be done with the help of Sokhotski-Wiestrass formula, but this time both the real parts and imaginary parts of Π_{00} and Π_{11} become non-vanishing.

We focus on the *real parts* at the beginning. For the density-density component,

$$\begin{aligned}
\mathcal{R}e\,\Pi_{00} &= \mathcal{P}\int \frac{n_F(\xi_{\boldsymbol{p}})(1-n_F(\xi_{\boldsymbol{p}+\boldsymbol{q}}))}{\omega+\xi_{\boldsymbol{p}}-\xi_{\boldsymbol{p}+\boldsymbol{q}}} - \frac{(1-n_F(\xi_{\boldsymbol{p}}))n_F(\xi_{\boldsymbol{p}+\boldsymbol{q}})}{\omega+\xi_{\boldsymbol{p}}-\xi_{\boldsymbol{p}+\boldsymbol{q}}}\frac{\mathrm{d}^2p}{(2\pi)^2} \\
&= \mathcal{P}\int \frac{n_F(\xi_{\boldsymbol{p}})}{\omega+\xi_{\boldsymbol{p}}-\xi_{\boldsymbol{p}+\boldsymbol{q}}} - \frac{n_F(\xi_{\boldsymbol{p}+\boldsymbol{q}})}{\omega+\xi_{\boldsymbol{p}}-\xi_{\boldsymbol{p}+\boldsymbol{q}}}\frac{\mathrm{d}^2p}{(2\pi)^2}
\end{aligned}$$

$$= \mathcal{P}\int \frac{n_F(\xi_{\boldsymbol{p}})}{\omega+\xi_{\boldsymbol{p}}-\xi_{\boldsymbol{p}+\boldsymbol{q}}} - \frac{n_F(\xi_{\boldsymbol{p}})}{\omega+\xi_{\boldsymbol{p}-\boldsymbol{q}}-\xi_{\boldsymbol{p}}}\frac{\mathrm{d}^2p}{(2\pi)^2} \equiv \mathcal{R}e(\Pi_{00})^- - \mathcal{R}e(\Pi_{00})^+, \tag{C.6}$$

with

$$\mathcal{R}e(\Pi_{00})^\pm = \mathcal{P}\int_{p<p_F} \frac{2m}{2m\omega \pm q^2 - 2pq\cos\theta}\frac{\mathrm{d}^2p}{(2\pi)^2}.$$

Likewise, since no confinement is imposed on angle variable, we direct have (denoting $q_\pm^2 \equiv 2m\omega \pm q^2$)

$$\mathcal{R}e(\Pi_{00})^\pm = \frac{m}{2\pi^2}\int_{p<p_F} p\,\mathrm{d}p\int_0^{2\pi}\frac{\mathrm{d}\theta}{q_\pm^2 - 2pq\cos\theta} = \frac{m}{\pi}\int_{p<pF,p<|q_\pm^2|/2q}\frac{p\,\mathrm{sgn}(q_\pm^2)}{\sqrt{|q_\pm^2|^2-4p^2q^2}}\,\mathrm{d}p.$$

For our case $|\boldsymbol{q}| \ll p_F, \omega \ll \frac{qp_F}{m}$ the confinement on integral domain can be unified as the simple $p < \frac{|q_\pm^2|}{2q}$ since

$$q \ll p_F \bigcap \frac{m\omega}{q} \ll p_F \implies \frac{|q_\pm^2|}{2q} = \left|\frac{m\omega}{q} \pm \frac{q}{2}\right| \ll p_F.$$

So

$$\mathcal{R}e(\Pi_{00})^\pm = \frac{m}{\pi}\int_{p<|q_\pm^2|/2q}\frac{p\,\mathrm{sgn}(q_\pm^2)}{\sqrt{|q_\pm^2|^2-4p^2q^2}}\,\mathrm{d}p = \frac{mq_\pm^2}{4\pi q^2}, \tag{C.7}$$

and by (C.6) we finally get[①]

$$\mathcal{R}e\,\Pi_{00}(\boldsymbol{q},\omega) = \frac{m}{4\pi q^2}\left(2m\omega - q^2 - 2m\omega - q^2\right) = \frac{m}{2\pi}, \tag{C.8}$$

which is in accordance with the results under static limit we obtained before.

Ditto for the procedure of density-density component, with slight changes we can direct write down the final integral of the real part of the current-current correlation function

$$\mathcal{R}e(\Pi_{11})^\pm = \frac{m}{\pi}\int_{p<|q_\pm^2|/2q}\frac{e^2p^2}{m^2}\frac{p\,\mathrm{sgn}(q_\pm^2)}{\sqrt{|q_\pm|^2-4p^2q^2}}\,\mathrm{d}p = \frac{q_\pm^6}{24\pi m q^4}. \tag{C.9}$$

Thus

$$\begin{aligned}\mathcal{R}e\,\Pi_{11}(\boldsymbol{q},\omega) &= \frac{1}{24\pi m q^4}\left((2m\omega-q^2)^3 - (2m\omega+q^2)^3\right) = \frac{1}{24\pi m q^4}(-q^6 - 24m^2\omega^2q^2) \\ &= -\frac{q^2}{12\pi m} - \frac{m\omega^2q^2}{\pi},\end{aligned} \tag{C.10}$$

[①]Obviously this result is *accurate with no approximation*, so the series expansion expression in HLR's work is to some extent wrong.

which reduces to (C.5) at the static limit $\omega = 0$, as is expected.

Next we turn to focus on the *imaginary parts*.

$$\begin{aligned}\mathcal{I}m\,\Pi_{00} &= (-\pi)\int\Big(n_F(\xi_{\boldsymbol{p}})(1-n_F(\xi_{\boldsymbol{p}+\boldsymbol{q}}))+(n_F(\xi_{\boldsymbol{p}})-1)n_F(\xi_{\boldsymbol{p}+\boldsymbol{q}})\Big)\delta(\omega+\xi_{\boldsymbol{p}}-\xi_{\boldsymbol{p}+\boldsymbol{q}})\frac{\mathrm{d}p^2}{(2\pi)^2}\\ &= (-\pi)\int(n_F(\xi_{\boldsymbol{p}})-n_F(\xi_{\boldsymbol{p}+\boldsymbol{q}}))\delta(\omega+\xi_{\boldsymbol{p}}-\xi_{\boldsymbol{p}+\boldsymbol{q}})\frac{\mathrm{d}p^2}{(2\pi)^2}\\ &= \frac{-1}{4\pi}\int_0^{p_F}p\,\mathrm{d}p\int_0^{2\pi}\mathrm{d}\theta\,\Theta(\xi_{\boldsymbol{p}+\boldsymbol{q}}-\mu)\times\delta\left(\omega+\frac{\boldsymbol{q}^2}{2m}-\frac{(\boldsymbol{p}+\boldsymbol{q})^2}{2m}\right)\mathrm{d}p^2.\end{aligned} \tag{C.11}$$

Let $x \equiv |\boldsymbol{p}+\boldsymbol{q}|$, then $x^2 = p^2+q^2+2pq\cos\theta$ and

$$\begin{aligned}2x\,\mathrm{d}x = 2pq\sin\theta\,\mathrm{d}\theta &= 2pq\sqrt{1-\frac{(p^2+q^2-x^2)^2}{4pq}}\,\mathrm{d}\theta\\ \Longrightarrow\ \mathrm{d}\theta &= \frac{2x\,\mathrm{d}x}{\sqrt{x^2-(p-q)^2}\sqrt{(p+q)^2-x^2}}.\end{aligned}$$

Hence[①]

$$\mathcal{I}m\,\Pi_{00} = \frac{-1}{2\pi}\int_0^{p_F}p\,\mathrm{d}p\times 2\int_{|p-q|}^{|p+q|}\mathrm{d}x\frac{x\Theta(x-p_F)\,\delta\left(\omega-\frac{x^2}{2m}+\frac{p^2}{2m}\right)}{\sqrt{(x^2-(p-q)^2)((p+q)^2-x^2)}}.$$

There is only one zero point in delta function $x_0 = \sqrt{2m\omega+p^2}$ since $x>0$, so integral of x can be performed directly

$$\begin{aligned}\mathcal{I}m\,\Pi_{00} &= \frac{-1}{2\pi}\int_0^{p_F}p\,\mathrm{d}p\times 2\int_{|p-q|}^{|p+q|}\mathrm{d}x\,\frac{x\Theta(x-p_F)\delta(x-x_0)}{\left|\frac{-x_0}{m}\right|\sqrt{(x^2-(p-q)^2)((p+q)^2-x^2)}}\\ &= \frac{m}{\pi}\int_0^{p_F}\frac{p\,\mathrm{d}p}{\sqrt{4p^2q^2-(2m\omega-q^2)^2}}\end{aligned} \tag{C.12}$$

with $x_0 > p_F$ as well as $|p-q| < x_0 < |p+q|$, which is equivalent to

$$p > p_a \equiv \sqrt{p_F^2-2m\omega},\quad q^2-2pq < 2m\omega < q^2+2pq.$$

And the latter inequality can be unified as

$$p > p_b \equiv \left|\frac{m\omega}{q}-\frac{q}{2}\right|.$$

The integral domain is determined by maximum between p_a and p_b, i.e., $p_{\text{min}} = \max(p_a, p_b)$. But in our situation, $p_a > p_b$ always holds because both $\frac{m\omega}{q}$ and $\frac{q}{2}$ are far less than p_F and then

$$p_b^2-p_a^2 = \left(\frac{m\omega}{q}+\frac{q}{2}\right)^2-p_F^2 \sim -p_F^2 < 0.$$

[①]The extra factor 2 comes from the integral range of θ.

Therefore, the integral (C.12) can be evaluated as

$$
\begin{aligned}
\mathcal{I}m\,\Pi_{00} &= \frac{m}{\pi}\int_{p_a}^{p_F}\frac{p\,\mathrm{d}p}{\sqrt{4p^2q^2-(2m\omega-q^2)^2}} \\
&= \frac{mp_F}{2\pi q}\left[\sqrt{1-\frac{1}{4p_F^2}\left(q-\frac{2m\omega}{q}\right)^2}-\sqrt{1-\frac{1}{4p_F^2}\left(q+\frac{2m\omega}{q}\right)^2}\right] \\
&= \frac{m^2\omega}{2\pi q p_F}+\mathcal{O}\left(q^4,\left(\frac{\omega}{q}\right)^4\right). \qquad \text{(C.13)}
\end{aligned}
$$

Likewise, with slight changes of above discussions we can direct write down the final integral of the imaginary part of the current-current correlation function

$$
\begin{aligned}
\mathcal{I}m\,\Pi_{11} &= \frac{m}{\pi}\int_{p_a}^{p_F}\frac{e^2p^2}{m^2}\frac{p\,\mathrm{d}p}{\sqrt{4p^2q^2-(2m\omega-q^2)^2}} \\
&= \frac{1}{24\pi m q^4}\left\{\left((q^2-2m\omega)^2+2p_F^2q^2\right)\left(\sqrt{1-\left(\frac{q^2-2m\omega}{2p_Fq}\right)^2}\right.\right. \\
&\qquad \left.\left.-\sqrt{1-\left(\frac{q^2+2m\omega}{2p_Fq}\right)}\right)+4m\omega q^2\sqrt{1-\left(\frac{q^2-2m\omega}{2p_Fq^2}\right)^2}\right\} \\
&\sim \frac{p_F}{12\pi m q^3}\left\{\left((q^2-2m\omega)^2+2p_F^2q^2\right)\left[1-\frac{1}{2}\left(\frac{q^2-2m\omega}{2p_Fq}\right)^2-1\right.\right. \\
&\qquad \left.+\frac{1}{2}\left(\frac{q^2-2m\omega}{2p_Fq}\right)^2+\mathcal{O}\left(q^2,\left(\frac{m\omega}{q}\right)^2\right)\right] \\
&\qquad \left.+4m\omega q^2\left[1-\frac{1}{2}\left(\frac{q^2+2m\omega}{2p_Fq}\right)^2+\mathcal{O}\left(q^2,\left(\frac{m\omega}{q}\right)^2\right)\right]\right\} \\
&= \frac{p_F}{12\pi m}\left\{\left[(q^2-2m\omega)^2+2p_F^2q^2\right]\frac{m\omega}{p_F^2q^3}+\frac{4m\omega}{q}\right. \\
&\qquad \left.-\frac{2m\omega}{q}\left(\frac{q^2+2m\omega}{2p_Fq}\right)^2+\mathcal{O}\left(q^3,\left(\frac{m\omega}{q}\right)^3\right)\right\} \\
&= \frac{p_F}{12\pi m}\left[\frac{6m\omega}{q}+\mathcal{O}\left(q^3,\left(\frac{m\omega}{q}\right)^3\right)\right]\sim\frac{p_F\omega}{2\pi q}. \qquad \text{(C.14)}
\end{aligned}
$$

To sum up, we have[①]

$$
\begin{cases}
\Pi_{00}(\boldsymbol{q},\omega)=\dfrac{m}{2\pi}\left(1+i\dfrac{\omega}{qv_F}\right)+\cdots, \\[2ex]
\Pi_{11}(\boldsymbol{q},\omega)=-\dfrac{q^2}{12\pi m}+\dfrac{i\omega}{q}\dfrac{2n_e}{p_F}+\cdots.
\end{cases}
\qquad \text{(C.15)}
$$

[①]Recall that $p_F=\sqrt{4\pi n_e}$. The diamagnetic term $\frac{-n_e}{m}$ in polarization tensor is canceled out by the integral of both retarded or advanced green functions, cf. [42, 65] for details.

The imaginary part of Π_{00} is small in contrast to the real part for $\omega \ll qp_F/m$ (clearly $\mathcal{I}m\,\Pi_{00} \sim \mathcal{O}(1/p_F^2)$), and thus can be neglected, while on the other hand, the imaginary part of Π_{11} is comparable to the real part. Finally we are left with

$$\mathbf{\Pi} = \begin{pmatrix} \frac{m}{2\pi} & 0 \\ 0 & -\frac{q^2}{12\pi m} + \frac{i\omega}{q}\frac{2n_e}{p_F} \end{pmatrix} \tag{C.16}$$

and thus[①]

$$\det(\mathbf{\Pi} + \boldsymbol{C}) \sim \frac{in_e}{\pi}\frac{\omega}{qv_F} - \frac{q^2}{(\phi_0\widetilde{\phi})^2}\left(1 + \frac{\widetilde{\phi}^2}{6} + \frac{mv(q)}{2\pi}\right),$$

where we have insert the expression of $\widetilde{\phi}_0 = \frac{2\pi}{e}$. Different from the situation of Fermi liquid, there is a pole called "overdamped mode" locating at the imaginary frequency

$$\omega \sim iq^3 v(q) \tag{C.17}$$

which represents the relaxation of density fluctuation.

C.3 Large Frequency $\omega \gg qk_F/m$

The case of high frequency is deviated from our mainline, so I omit the computation details here and direct list the polarization tensor below.

$$\begin{cases} \Pi_{00}(\boldsymbol{q}, \omega) \sim \dfrac{-n_e}{m}\dfrac{q^2}{\omega^2}, \\ \Pi_{11}(\boldsymbol{q}, \omega) \sim \dfrac{-n_e}{m} + \mathcal{O}(q^2). \end{cases} \tag{C.18}$$

Obviously the determinant of the matrix

$$(\mathbf{\Pi} + \boldsymbol{C}) \sim \begin{pmatrix} \dfrac{-n_e q^2}{m\omega^2} & \dfrac{-iq}{\phi_0\widetilde{\phi}} \\ \dfrac{iq}{\phi_0\widetilde{\phi}} & \dfrac{-n_e}{m}. \end{pmatrix}$$

vanishes at

$$\pm\omega_c = \frac{\phi_0 n_e \widetilde{\phi}}{m}, \tag{C.19}$$

we thus obtain the pole of $K_{\mu\nu}$ at $\omega = \omega_c$. This *cyclotron frequency* is accurately in consistency with the celebrated *Kohn's Theorem* [66], claiming that [59] **the cyclotron resonance of *Galilean-invariant* 2DEG lies exactly at the cyclotron frequency ω_c without any renormalizations due to interactions.**

[①] We concern about the determinate because of the expression of $\boldsymbol{K}$.

Bibliography

[1] Von Klitzing K, Dorda G, Pepper M. New method for high-accuracy determination of the fine-structure constant based on quantized hall resistance. *Physical Review Letters*, 1980, 45 (6): 494.

[2] Von Klitzing K. The quantized hall effect. *Reviews of Modern Physics*, 1986, 58(3): 519.

[3] Comtet A, Jolicoeur T, Ouvry S, et al. Aspects topologiques de la physique en basse dimension. topological aspects of low dimensional systems: volume 69. Springer Science & Business Media, 2000.

[4] Tsui D C, Stormer H L, Gossard A C. Two-dimensional magnetotransport in the extreme quantum limit. *Physical Review Letters*, 1982, 48(22): 1559.

[5] Stormer H L, Tsui D C, Gossard A C. The fractional quantum hall effect. *Reviews of Modern Physics*, 1999, 71(2): S298.

[6] Laughlin R B. Anomalous quantum hall effect: an incompressible quantum fluid with fractionally charged excitations. *Physical Review Letters*, 1983, 50(18): 1395.

[7] Tong D. Lectures on the quantum hall effect. *arXiv preprint arXiv:1606.06687*, 2016.

[8] Simon S H. The chern-simons fermi liquid description of fractional quantum hall states// Composite Fermions: A Unified View of the Quantum Hall Regime. World Scientific, 1998: 91-194.

[9] Zhang Y, Tan Y W, Stormer H L, et al. Experimental observation of the quantum hall effect and berry's phase in graphene. *nature*, 2005, 438(7065): 201.

[10] Gusynin V, Sharapov S. Unconventional integer quantum hall effect in graphene. *Physical review letters*, 2005, 95(14): 146801.

[11] Herbut I F. Theory of integer quantum hall effect in graphene. *Physical Review B*, 2007, 75 (16): 165411.

[12] Sarma S D, Adam S, Hwang E, et al. Electronic transport in two-dimensional graphene. *Reviews of Modern Physics*, 2011, 83(2): 407.

[13] Du X, Skachko I, Duerr F, et al. Fractional quantum hall effect and insulating phase of dirac electrons in graphene. *Nature*, 2009, 462(7270): 192.

[14] Dean C, Young A, Cadden-Zimansky P, et al. Multicomponent fractional quantum hall effect in graphene. *Nature Physics*, 2011, 7(9): 693.

[15] Ki D K, Fal' ko V I, Abanin D A, et al. Observation of even denominator fractional quantum hall effect in suspended bilayer graphene. *Nano letters*, 2014, 14(4): 2135-2139.

[16] Jain J K. Composite-fermion approach for the fractional quantum hall effect. *Physical review*

letters, 1989, 63(2): 199.

[17] Zhang S C, Hansson T H, Kivelson S. Effective-field-theory model for the fractional quantum hall effect. *Physical review letters*, 1989, 62(1): 82.

[18] Wilczek F. Fractional statistics and anyon superconductivity: volume 5. World scientific, 1990.

[19] Chen Y H, Wilczek F, Witten E, et al. On anyon superconductivity. *International Journal of Modern Physics B*, 1989, 3(07): 1001-1067.

[20] Lopez A, Fradkin E. Fractional quantum hall effect and chern-simons gauge theories. *Physical Review B*, 1991, 44(10): 5246.

[21] Fradkin E. Wave functionals for field theories and path integrals. *Nuclear Physics B*, 1993, 389(3): 587-600.

[22] Halperin B I, Lee P A, Read N. Theory of the half-filled landau level. *Physical Review B*, 1995, 47(12): 7312.

[23] Stern A, Halperin B I. Singularities in the fermi-liquid description of a partially filled landau level and the energy gaps of fractional quantum hall states. *Physical Review B*, 1995, 52(8): 5890.

[24] Haldane F, Rezayi E. Spin-singlet wave function for the half-integral quantum hall effect. *Physical review letters*, 1988, 60(10): 956.

[25] Read N, Green D. Paired states of fermions in two dimensions with breaking of parity and time-reversal symmetries and the fractional quantum hall effect. *Physical Review B*, 2000, 61 (15): 10267.

[26] Moore G, Read N. Nonabelions in the fractional quantum hall effect. *Nuclear Physics B*, 1991, 360(2-3): 362-396.

[27] Morf R H. Transition from quantum hall to compressible states in the second landau level: new light on the ν= 5/2 enigma. *Physical review letters*, 1998, 80(7): 1505.

[28] Suen Y, Engel L, Santos M, et al. Observation of a ν= 1/2 fractional quantum hall state in a double-layer electron system. *Physical review letters*, 1992, 68(9): 1379.

[29] Du R, Stormer H, Tsui D, et al. Experimental evidence for new particles in the fractional quantum hall effect. *Physical review letters*, 1993, 70(19): 2944.

[30] Lopez A, Fradkin E. Fermionic chern-simons theory for the fractional quantum hall effect in bilayers. *Physical Review B*, 1995, 51(7): 4347.

[31] Mandal S S, Ravishankar V. Theory of arbitrarily polarized quantum hall states: Filling fractions and wave functions. *Physical Review B*, 1996, 54(12): 8688.

[32] Modak S, Mandal S S, Sengupta K. Fermionic chern-simons theory of su (4) fractional quantum hall effect. *Physical Review B*, 2011, 84(16): 165118.

[33] Pyatkovskiy P, Gusynin V. Dynamical polarization of graphene in a magnetic field. *Physical Review B*, 2011, 83(7): 075422.

[34] Ni Z H, Yu T, Lu Y H, et al. Uniaxial strain on graphene: Raman spectroscopy study and band-gap opening. *ACS nano*, 2008, 2(11): 2301-2305.

[35] Farjam M, Rafii-Tabar H. Comment on "band structure engineering of graphene by strain: First-principles calculations". *Physical Review B*, 2009, 80(16): 167401.

[36] Manes J L. Symmetry-based approach to electron-phonon interactions in graphene. *Physical Review B*, 2007, 76(4): 045430.

[37] Neto A C, Guinea F, Peres N M, et al. The electronic properties of graphene. *Reviews of modern physics*, 2009, 81(1): 109.

[38] Castro-Villarreal P, Ruiz-Sánchez R. Pseudomagnetic field in curved graphene. *Physical Review B*, 2017, 95(12): 125432.

[39] Guinea F, Katsnelson M, Geim A. Energy gaps and a zero-field quantum hall effect in graphene by strain engineering. *Nature Physics*, 2010, 6(1): 30.

[40] Verbiest G, Brinker S, Stampfer C. Uniformity of the pseudomagnetic field in strained graphene. *Physical Review B*, 2015, 92(7): 075417.

[41] Bernevig B A, Zhang S C. Quantum spin hall effect. *Physical Review Letters*, 2006, 96(10): 106802.

[42] Altland A, Simons B D. Condensed matter field theory. Cambridge University Press, 2010.

[43] Fu L, Kane C L. Topological insulators with inversion symmetry. *Physical Review B*, 2007, 76(4): 045302.

[44] Goerbig M. Electronic properties of graphene in a strong magnetic field. *Reviews of Modern Physics*, 2011, 83(4): 1193.

[45] Tőke C, Lammert P E, Crespi V H, et al. Fractional quantum hall effect in graphene. *Physical Review B*, 2006, 74(23): 235417.

[46] Tőke C, Jain J K. Su (4) composite fermions in graphene: Fractional quantum hall states without analog in gaas. *Physical Review B*, 2007, 75(24): 245440.

[47] Nagaosa N. Quantum field theory in strongly correlated electronic systems. Springer Science & Business Media, 1999.

[48] Bolotin K I, Ghahari F, Shulman M D, et al. Observation of the fractional quantum hall effect in graphene. *Nature*, 2009, 462(7270): 196.

[49] Nomura K, MacDonald A H. Quantum hall ferromagnetism in graphene. *Physical Review Letters*, 2006, 96(25): 256602.

[50] Goerbig M O, Moessner R, Douçot B. Electron interactions in graphene in a strong magnetic field. *Physical Review B*, 2006, 74(16): 161407.

[51] Apalkov V M, Chakraborty T. Fractional quantum hall states of dirac electrons in graphene. *Physical review letters*, 2006, 97(12): 126801.

[52] Wen X g, Zee A. Classification of abelian quantum hall states and matrix formulation of topological fluids. *Physical Review B*, 1992, 46(4): 2290.

[53] Rajaraman R. Generalized chern-simons theory of composite fermions in bilayer hall systems. *Physical Review B*, 1997, 56(11): 6788.

[54] Nagaosa N. Quantum field theory in condensed matter physics. Springer Science & Business Media, 2013.

[55] Peskin M E. An introduction to quantum field theory. Westview press, 1995.

[56] Stratonovich R L. On a method of calculating quantum distribution functions. *Soviet Physics Doklady*, 1957, 2: 416.

[57] Hubbard J. Calculation of partition functions. *Physical Review Letters*, 1959, 3(2): 77.

[58] Abrikosov A A, Gorkov L P, Dzyaloshinski I E. Methods of quantum field theory in statistical physics. Courier Corporation, 2012.

[59] Fradkin E. Field theories of condensed matter physics. Cambridge University Press, 2013.

[60] Mahan G D. Many-particle physics. Springer Science & Business Media, 2013.

[61] Peterson M R, Nayak C. Effects of landau level mixing on the fractional quantum hall effect in monolayer graphene. *Physical review letters*, 2014, 113(8): 086401.

[62] Peterson M R, Nayak C. More realistic hamiltonians for the fractional quantum hall regime in gaas and graphene. *Physical Review B*, 2013, 87(24): 245129.

[63] Son D T. Is the composite fermion a dirac particle? *Physical Review X*, 2015, 5(3): 031027.

[64] Fräßdorf C. Abelian chern-simons theory for the fractional quantum hall effect in graphene. *Physical Review B*, 2018, 97(11): 115123.

[65] Sadovskii M V. Diagrammatics: lectures on selected problems in condensed matter theory. World Scientific, 2006.

[66] Kohn W. Cyclotron resonance and de haas-van alphen oscillations of an interacting electron gas. *Physical Review*, 1961, 123(4): 1242.